Current Research in Food Science 8 (2024) 100746

Contents lists available at ScienceDirect

Current Research in Food Science

journal homepage: www.sciencedirect.com/journal/current-research-in-food-science

Hemp (*Cannabis sativa* L.) protein: Impact of extraction method and cultivar on structure, function, and nutritional quality

Laura Eckhardt [a], Fan Bu [a], Adam Franczyk [b], Tom Michaels [c], Baraem P. Ismail [a,*]

[a] Department of Food Science and Nutrition, University of Minnesota, Saint Paul, MN, 55108, USA
[b] Department of Food and Human Nutritional Sciences, University of Manitoba, Winnipeg, MB, R3T 2N2, Canada
[c] Department of Horticultural Science, University of Minnesota, Saint Paul, MN, 55108, USA

ARTICLE INFO

Handling Editor: Dr. Xing Chen

Keywords:
Hemp protein isolate
Structural characteristics
Functional properties
Nutritional quality
Hemp protein extraction

ABSTRACT

Hemp (*Cannabis sativa* L.) is increasingly gaining traction as a novel and sustainable source of plant protein. Accordingly, the aim of this study was to investigate the effectiveness of two protein extraction methods, alkaline extraction coupled with isoelectric precipitation (AE-IEP) and salt extraction coupled with ultrafiltration (SE-UF) in producing hemp protein isolates (pH-HPI and salt-HPI) with high purity and yield. Structural characterization as impacted by extraction method and cultivar was performed and related to functional performance and nutritional quality. Both extraction methods, with carefully selected parameters, resulted in HPI with high purity (86.6–88.1% protein) and protein extraction yields (81.6–87.3%). All HPI samples had poor solubility (~9–20%) at neutral pH compared to commercial soy protein and pea protein isolates (cSPI, cPPI). A relatively high surface hydrophobicity and low surface charge contributed to such poor solubility of HPI. However, HPI demonstrated similar solubility at acidic pH (50–67%) and comparable gel strength (up to 24 N) to cSPI. Comparing experimental amino acid composition to the theoretical amino acid distribution in hemp protein provided insights to the functional performance of the protein isolates. While pH-HPI demonstrated better functionality than salt-HPI, minimal structural, functional, and nutritional differences were noted among the pH-HPI samples extracted from four different cultivars. Overall, results from this work could be used to guide future attempts to further develop successful protein extraction processes, and to provide valuable insights to propel breeding efforts that target enhanced hemp protein characteristics for food applications.

1. Introduction

The global protein ingredients market, which was estimated at ~$78 billion in 2022, is predicted to grow at a compound annual growth rate (CAGR) of ~6% through 2030 (Grand View Research, 2023).While animal-derived proteins make up a significant portion of the global protein market (~80%), plant-derived proteins are gaining traction. In fact, the plant-based market has reached a value of $8 billion in the United States alone and has a CAGR of 9% (Grand View Research, 2023; SPINS/GFI, 2023). The spike in the plant proteins and plant-based foods market is mostly attributed to an increase in consumers who are choosing flexitarian, vegetarian, or vegan diets. The shift in diet trends is a consequence of a variety of reasons, including concerns about health, animal welfare, and the environment (Ismail et al., 2020).

Currently, soybeans are the predominant source of plant protein ingredients (Grand View Research, 2023). However, soy is mostly a GMO crop in the US and is one of the "Big 9" allergens identified by the Food and Drug Administration (FDA). Pea protein, as a replacement to soy protein, is witnessing rampant market growth, attributed to the agronomic benefits of growing pea, low production cost, low allergenicity, and acceptable functionality and nutritional quality (Barac et al., 2010; Grand View Research, 2023; Ismail et al., 2020). However, to meet the growing consumer demand for plant proteins, other novel sources must be explored.

Hemp (*Cannabis sativa* L.) oilseeds are among the promising plant protein sources. However, research on hemp oilseeds as a food source has been hindered by legal restrictions due the similarities of hemp to marijuana (Aluko, 2017; Callaway, 2004). Recently, legal restrictions on hemp cultivation and food use in North America were lifted, paving the way for the inclusion of hemp oilseeds and their products in food applications.

As is the case for other oilseeds, hemp oilseed meal remaining after

* Corresponding author. 1334 Eckles Avenue, Saint Paul, MN, 55108, USA.
E-mail address: bismailm@umn.edu (B.P. Ismail).

https://doi.org/10.1016/j.crfs.2024.100746
Received 30 January 2024; Received in revised form 31 March 2024; Accepted 17 April 2024
Available online 19 April 2024

oil extraction contains an appreciable amount of highly digestible protein (approximately 40–60% protein) with a favorable amino acid profile (Callaway, 2004; House et al., 2010). Milled into flour, the defatted hemp meal has been sold directly to consumers as a dietary hemp protein powder (House et al., 2010). However, protein purification to produce a functional hemp protein isolate (HPI) could extend the use of hemp protein to a wide range of food applications.

Different protein extraction and purification methods have been investigated to produce HPI. The most tested method is alkaline extraction coupled with isoelectric precipitation (AE-IEP). Typically for defatted hemp meal, this method involves solubilization of the protein at pH 10 followed by precipitation around pH 5 to further purify the protein (Girgih et al., 2014; Hadnađev et al., 2018; M. Liu et al., 2023; X. Liu et al., 2023; Shen et al., 2020). While the reported protein purity was considerably high (>80%), the protein yields were modest, typically between 30 and 50% (Hadnađev et al., 2018; Shen et al., 2020). A yield of approximately 80% was achieved only when using a highly alkaline solution (KOH or NaOH, pH 13) for protein solubilization. This very high alkalinity led to protein structural damage that most likely contributed to severely reduced functionality (Cabral et al., 2022).

The inefficiency of hemp protein extractions suggests that greater efforts should be devoted to the hemp protein isolation process. In our previous studies, the solubilization pH and the number of solubilization (i.e., solvent replenishment) had a pronounced impact on both the protein yield and the structure and functionality of pea and chickpea proteins (Hansen et al., 2022; Yaputri et al., 2023). In addition, reduction of fat content to below 3% contributed to enhanced protein extraction efficiency (Yaputri et al., 2023). Such efforts as applied to defatted hemp meal are lacking in literature.

Another major drawback that has been reported when producing HPI via AE-IEP is an unappealing, offensive brown or greenish color (Hadnađev et al., 2018; Helstad et al., 2022). Hemp hulls contain phenolic compounds, which can interact with the protein during extraction resulting in reduced protein solubility. Additionally, these phenolic compounds become oxidized under the high alkalinity used during the extraction of hemp protein, contributing to the dark, greenish color of HPI. Such an offensive color would decrease consumers' acceptance and limit the use of HPI in food applications. Therefore, dehulling prior to defatting and protein extraction should be further evaluated as a preparatory step for the production of HPI with acceptable color and protein properties.

Salt extraction coupled with ultrafiltration (SE-UF) is another protein extraction and purification method that has been investigated for the production of HPI. Previous studies on pea protein showed that SE-UF contributed to better functional properties than AE-IEP (Hansen et al., 2022). While SE-UF resulted in HPI with high protein purity and higher yield than AE-IEP, the reported protein yield relatively remained low (<50%) (Dapčević-Hadnađev et al., 2018; Hadnađev et al., 2018; Malomo and Aluko, 2015a). Furthermore, SE-UF has not been as thoroughly investigated in direct comparison to AE-IEP for the production of HPI.

Other than protein purity and yield, the extraction and purification method impacts the protein's structural and functional properties (Hansen et al., 2022; Mitacek et al., 2023). Research on hemp protein functionality, while not robust, has shown limitations in solubility, water binding, emulsification, and foaming properties (House et al., 2010; Potin and Saurel, 2020; Tang et al., 2006). Information on the water holding capacity and gelation properties of hemp protein is scarce. Functionality is heavily influenced by the protein structure, which has only been moderately explored for hemp protein. While there are some reports on hemp protein characteristics, the information is far from being sufficient or relevant to selecting an extraction method for hemp protein that contributes to favorable structural and functional properties. Comparison of HPI to common plant protein ingredients, such as soy and pea protein isolates produced under similar extraction conditions, is also lacking in literature.

Furthermore, literature lacks information on hemp protein nutritional properties, including digestibility and essential amino acids, as impacted by the extraction method. Hemp seed protein contains all of the essential amino acids and can be easily digested (House et al., 2010). However, hemp protein is deficient in lysine, an essential amino acid, causing it to be nutritionally inferior to soy and pea protein. Therefore, evaluating protein digestibility and amino acid score as impacted by the protein extraction method is essential.

Equally important is the impact of varietal differences on the protein characteristics as noted widely for soy and pea protein (Casey et al., 1982; Mertens et al., 2012; Pesic et al., 2005). Hemp oilseeds from different cultivars varied in crude protein content (19.5–35.6%) and in amino acid profile (Galasso et al., 2016; House et al., 2010; Irakli et al., 2019; Pannico et al., 2022; Vonapartis et al., 2015). However, differences in protein profile, structure, and functionality among different hemp cultivars are only minimally explored relative to other species. Identifying differences in hemp protein among cultivars can be leveraged for breeding efforts to improve protein functionality for food applications. Additionally, there has been no bioinformatics analysis of the various variants of 11S and 7S globulins present in HPI. Such an analysis could offer valuable insights to steer breeding efforts.

Therefore, the objectives of this study were to 1) investigate different protein extraction conditions, following AE-IEP and SE-UF, to produce HPI with acceptable color, purity, yield, structural and functional characteristics, and nutritional quality, 2) evaluate HPI produced from four industrial cultivars for differences in color, protein extraction yield, and protein structural, functional, and nutritional properties, 3) analyze the sequences of different variants of 11S and 7S globulins in the protein database, assessing both sequence similarity and amino acid compositions, and subsequently compared these results to our experimental amino acid composition.

2. Materials and methods

2.1. Materials

Whole hemp seeds from the cultivar CFX-2 harvested in 2016 were kindly provided by Hemp Acres (Waconia, MN, USA), and CFX-2, Grandi, Joey, and Picolo harvested in 2019 were kindly provided by Hemp Genetics International (North Saskatoon, SK, Canada). Commercial soy protein isolate (cSPI, ProFam 974, 90.1% protein, 4.2% ash) and pea protein isolate (cPPI, ProFam 580, 79.5% protein, 5.6% ash) were kindly provided by Archer Daniels Midland (ADM) (Decatur, IL, USA). All samples were stored in closed containers sealed with Parafilm at −20 °C when not in use. SnakeSkin™ dialysis tubing with a molecular weight cut-off of 3.5 kDa and Sartorius Vivaflow™ 200 Crossflow Cassettes for membrane filtration with a molecular weight cut-off of 3 kDa were purchased from Thermo Fischer Scientific™ (Waltham, MA, USA). Criterion™ TGX™ 4–20% precast gels (18 wells), 10X tris/glycine/sodium dodecyl sulfate (SDS) running buffer, Laemmli sample buffer, Precision Plus™ molecular weight marker, and Imperial™ Protein Stain were purchased from Bio-Rad Laboratories, Inc. (Hercules, CA, USA). Electrophoresis grade sodium dodecyl sulfate (SDS), 2-mercaptoethanol (βME), 8-anilino-1-napthalenesulfonic acid ammonium salt (ANS), and Celatom® (C8656) were purchased from Sigma-Aldrich (St. Louis, MO, USA). Trypsin (T0303; from porcine pancreas Type IX-S, lyophilized powder, 13,000–20,000 BAEE units/mg protein), α-chymotrypsin (C4129; from bovine pancreas C4129 Type II, lyophilized powder, P40 units/mg protein), and protease (P5147; from *Streptomyces griseus* Type XIV, P3.5 units/mg solids) were used for protein digestibility assay and were purchased from Sigma-Aldrich. Casein (400601, high nitrogen, 80 mesh) for use as a reference in the protein digestibility assay was purchased from Dyets Inc. (Bethlehem, PA, USA). All other chemicals and reagents of analytical grade quality were purchased from Thermo Fischer Scientific or Sigma-Aldrich.

2.2. Production of defatted hemp meal (DHM)

Hemp seeds were dehulled using an industrial-scale huller (Bühler MHSA huller, Bühler, Uzwil, Switzerland). Hull pieces were separated from hemp seeds using multiple sieves, a grain aerator, and a small-scale gravity separator table (Whippet V.80 Gravity Separator Table, Sutton, Steele & Steele, Inc., Dallas, TX, USA). Manual separation using forceps was employed to remove residual hull pieces. Dehulled seeds were pressed using a hydraulic press (Carver Model C 8-ton manual bench top laboratory press with 2094 cage equipment, Carver Inc., Wabash, IN, USA) for 28–30 h at ambient temperature with a maximum pressure of 16,000 psi. The pressed hemp cake was ground using a KitchenAid® coffee grinder (KitchenAid, Benton Harbor, MI, USA). The ground cake was defatted using hexane in a ratio of 3:1 (hexane to hemp seeds) under constant agitation for 1-h, followed by another 30-min cycle with fresh solvent. Defatted cake was left overnight under the hood to evaporate off any residual hexane before milling to 50-mesh using a cyclone sample mill (UDY Corp, Fort Collins, CO, USA). Defatted, milled hemp meal had less than 3.5% fat on wet basis as determined following the Mojonnier AOAC method 922.06. The protein content (~60% protein) of the defatted hemp meal (DHM) was determined by the Dumas AOAC method 990.03 using a nitrogen analyzer (LECO, St. Joseph, MI, USA) and a protein conversion factor of 5.30 (USDA, 2018).

2.3. pH extraction of hemp protein

2.3.1. Preliminary screening of protein solubilization pH

To select pH extraction conditions, different protein solubilization pHs were tested (pH 7, 8, 9, 10, 11, 12). DHM from CFX-2 2016 was solubilized, in triplicate, in double distilled water (DDW, 5% total solids), adjusted to the desired pH (using 2M NaOH), for 1 h at room temperature at a certain pH. After centrifugation, the supernatant was decanted, and the weight recorded. The protein content of the supernatant was determined following the Dumas method and was used to calculate the weight in grams of protein in the supernatant. The starting protein weight in grams and the grams of protein in the total supernatant were used to determine the percent of soluble protein at each pH (i.e., the protein yield).

2.3.2. Selection of pH extraction conditions

DHM from CFX-2 2016 was used to produce HPI using AE-IEP, coupled with a double solubilization method (Hansen et al., 2022; Mitacek et al., 2023). In triplicate, DHM was fully dispersed in DDW at 5% total solids. The pH was adjusted to 10 or 11 using 2 M NaOH and stirred for 1 h at room temperature. The dispersions were centrifuged at 12,000×*g* for 15 min, and the supernatants were collected and neutralized. Then, each pellet was redispersed in water (5% total solids) with the pH readjusted to pH 10 or 11 followed by stirring for another. After centrifugation, the supernatant was combined with the first supernatant and neutralized. Each residual pellet was collected and lyophilized for mass balance determination. The pH of the combined supernatants was adjusted to pH 5 with 2 M HCl, followed by centrifugation at 12,000×*g* for 10 min. The supernatant was collected and lyophilized for mass balance determination, while the protein pellet was redispersed (1:4 w/w) in DDW and adjusted to pH 7.0 with 2 M NaOH, followed by dialysis and lyophilization. The protein content of the HPI, along with the residual pellet after protein solubilization and residual supernatant after protein precipitation, was determined following the Dumas method. Mass balance determination tracked the protein yield of the following fractions: HPI, the residual pellet after solubilization, and the residual supernatant after protein precipitation. The protein yield/lost/residue for each fraction was calculated. The ash content of each HPI was determined following the official AOAC 942.05 dry ashing method. The AE-IEP with select conditions was used to produce pH-HPI in sufficient amount from each cultivar for structural and functional characterization. The protein content of HPI produced from each cultivar (87.8–89.0% protein) was determined by the Dumas AOAC method with a conversion factor of 5.30. Protein extraction yields ranged from 81.4 to 82.4%.

2.4. Salt extraction of hemp protein

2.4.1. Preliminary screening of salt solubilization

To select salt concentration for solubilization of hemp protein, four salt concentrations were tested. In triplicate, DHM from CFX-2 2016 was dispersed at 5% total solids in salt (NaCl) solutions at different concentrations 0.5 M, 0.75 M, 1 M, and 1.25 M and stirred for 1 h in a water bath at 50 °C. Based on preliminary findings heating at 50 °C during the solubilization step resulted in a 25% increase in soluble protein compared to solubilization at room temperature. This observation was in accordance to reported enhancement of camelina protein extraction when salt solubilization was performed at 50 °C (Boyle et al., 2018). After centrifugation, supernatants were decanted, and the weights recorded. Percent soluble protein was determined as outlined in section 2.3.1.

2.4.2. Selection of salt extraction conditions

DHM from CFX-2 2016 was used to produce HPI using SE-UF, similar to the process outlined by (Hansen et al., 2022; Mitacek et al., 2023; Yaputri et al., 2023). Double solubilization was employed to enhance the yield, as was confirmed in previous reports. In triplicate, DHM was dispersed in 0.5 M or 0.75 M NaCl at 5% total solids and stirred for 1 h in a water bath at 50 °C. Dispersions were then centrifuged at 12,000×*g* for 20 min, and the supernatants were collected. Each pellet was resolubilized in 0.5 M or 0.75 M NaCl at 5% total solids and stirred for another hour at 50 °C. After centrifugation, the supernatant was combined with the first supernatant. Each pellet was saved and lyophilized for mass balance determination. The combined supernatants from each replicate were adjusted to pH 7 using 2 M NaOH or HCl and ultrafiltered using a lab scale Sartorius Vivaflow® 200 system with two membrane cassettes run side-by-side to increase efficiency. A peristaltic pump (Masterflex Easy Load Pump Head- Size 15, Masterflex Economy Drive Peristaltic Pump 230V, Sartorius) was used to push the protein solution across the membranes at a pressure of 2–2.5 bars. The retentate was recirculated to the feed container for additional washes (Hansen et al., 2022), while components with molecular weights smaller than 3 kDa passed through as permeate and were discarded. The retained protein solution was then dialyzed and lyophilized. The protein content of HPI and the discarded pellet was determined following the Dumas method. Mass balance determination tracked the protein yield of the following fractions: HPI and the residual pellet after solubilization. The protein yield/lost/residue for each fraction was calculated. The selected SE-UF conditions were used to produce salt-HPI in sufficient amounts from each cultivar in sufficient quantities for structural and functional characterization.

2.5. Color measurement

The color of all samples was measured in triplicate using a Chroma Meter CR-221 (Minolta Camera Co., Osaka, Japan). Prior to sample analysis, the colorimeter was calibrated using a white CR-221 calibration plate (Minolta). Equivalent amounts of sample were weighed out to obtain a similar thickness of sample for all readings. The color measurements were recorded using the CIE (International Commission on Illumination) 1976 L* a* b* color system, where L* indicates lightness on a scale from 0 (black) to 100 (white), a* indicates redness (positive value) and greenness (negative value), and b* indicates yellowness (positive value) and blueness (negative value).

2.6. Protein structural characterization

2.6.1. Protein profiling by gel electrophoresis

Protein profiling of all samples was performed using sodium dodecyl polyacrylamide gel electrophoresis (SDS-PAGE) as outlined by (Boyle et al., 2018). Briefly, samples were prepared under non-reducing conditions (in Laemmli buffer) and reducing (in Laemmli buffer with β-mercaptoethanol (βME), loaded (5 μL–50 μg protein) on 4–20% precast Tris-HCl gradient gels, electrophoresed, stained, and imaged using Molecular Imager Gel Doc XR system (Bio-Rad Laboratories).

2.6.2. Thermal denaturation by differential scanning calorimetry (DSC)

Denaturation temperature and enthalpy of denaturation were determined using a DSC instrument (DSC 1 STARe System, Mettler Toledo, Columbus, OH, USA) following the method outlined by Bu et al. (2022), with modifications in the starting and final measurement temperature. Protein samples were dispersed in DDW (20% protein, w/v) and equilibrated overnight at ambient temperature. An aliquot (20 μL) of each sample, in triplicate, was placed in an aluminum pan, sealed, and analyzed alongside an empty pan as a reference. The pans were kept at 25 °C for 5 min before ramping up the temperature at a rate of 5 °C per minute up to 115 °C. Thermograms were recorded, and peaks were integrated using the STARe Software version 11.00 (Mettler Toledo).

2.6.3. Protein surface properties

Surface hydrophobicity was determined for all samples using a spectrofluorometric method that utilizes 1-aniline-8-napthalene sulfonate (ANS) as outlined by Bu et al. (2022). The relative fluorescence index (RFI) was measured using a microplate reader (BioTek Synergy HT, BioTek Instruments, Winooski, VT, USA). The RFI was measured at excitation and emission wavelengths of 400/30 (wavelength/bandwidth) and 460/40 nM and 40 gain. Zeta potential was measured using a dynamic light scattering instrument, Malvern Nano Z-S Zetasizer, following the method outlined by Bu et al. (2022), with modifications in solubilization medium and number of measurements per sub-reading. Solutions were prepared, in triplicate, (0.1% protein, w/v) in DDW and solubilized for 2 h. Before each sample was analyzed, the pH was adjusted to 7.0. An aliquot (~1 mL) of each sample was inserted into a folded capillary cell and placed into the Zetasizer. The electrophoretic motility was measured by taking three sub-rep readings, each comprised of 20 measurements. Malvern's Zetasizer software (version 7.13) was used to determine zeta potential using the Smoluchowski model.

2.6.4. Protein secondary structures by attenuated total reflectance fourier transform infrared spectroscopy (ATR-FTIR)

ATR-FTIR spectra for each sample were recorded using Fourier transform infrared spectrometer (Thermofisher Nicolett iS50 FTIR) following the method outlined by Bu et al. (2023) and integration by Husband et al. (2024). The assignment of secondary structures, including α-helix, β-sheet, β-turn, and random coil, was conducted in accordance with the methodologies described in Sadat and Joye (2020) and Housmans et al. (2022).

2.7. Protein functional characterization

2.7.1. Protein solubility

The solubility of all samples was determined following the method outlined by (Boyle et al., 2018), with modifications in the solubilization medium and pH. Protein solubility in DDW as well as in 0.5 M NaCl was measured. Protein solubility was measured at neutral pH (pH 7) and at an acidic pH of 3.2 instead of 3.4. pH 3.2 was chosen as it is still within the range used in industrial applications for acidic beverages but is further away from hemp protein's isoelectric point than pH 3.4. In triplicate, protein dispersions (1% protein, w/v) in DDW and in 0.5 M NaCl were prepared, allowed to solubilize for 2 h, and pH adjusted to either pH 7.0 or 3.2. Both heated (80 °C for 30 min) and non-heated samples were centrifuged at 15,682×*g* for 10 min. Protein solubility was then determined as the percent of protein in the supernatant relative to the initial protein content of the solution.

2.7.2. Gel strength and water holding capacity (WHC)

Heat-induced gels was prepared and assessed as outlined by Boyle et al. (2018), with modifications in the solubilization medium and the texture analyzer probe speed. Protein solutions (15% protein, w/v) were prepared, in triplicate, either in DDW or 0.5 M NaCl, adjusted to pH 7.0, and solubilized for 2 h. The chosen protein concentration was based on determination of the least gelation concentration (LGC) (Boyle et al., 2018). Aliquots (1 mL) were heated at 95 °C (±2 °C) in a water bath for 10 (cSPI, pH-HPIs, salt-HPI) or 20 min (cPPI) and left to cool down to room temperature prior to analysis. Gel strength in Newtons (i.e., the maximum force that was needed to rupture the gel) was determined using a TA-TX Plus Texture Analyzer (Stable Micro Systems LTD, Surrey, UK) with a 100 mm diameter probe, a 5 mm s^{-1} test speed, and a target distance of 0.5 mm from the plate. To determine WHC, protein gels were prepared as stated above, however, they were centrifuged at 1000×*g* for 5 min and inverted for 10 min to drain water expelled from the gel. After 10 min, the weight of each gel was recorded. WHC was measured as the percentage of water physically entrapped in the gel matrix.

2.7.3. Emulsification capacity

Emulsification capacity (EC), express as g of oil emulsified by 1 g of protein, was determined following the method outlined by Boyle et al. (2018), with modifications in the solubilization medium. Protein solutions were prepared, in triplicate, in either DDW or 0.5 M NaCl at 1% protein (w/v) and solubilized for 2 h. After solubilization, the pH of the protein solutions was adjusted to 7.0 and corn oil was titrated while mixing using a homogenizer (IKA® RW 20 Digital; IKA Works Inc., Wilmington, NC, USA) with a four-blade, 50 mm diameter shaft (IKA® R 1342) rotating at 860–870 rpm. The oil titration and simultaneous homogenization continued until phase inversion occurred.

2.7.4. Emulsion stability and activity

Emulsification stability (ES) and activity index (EAI) were measured as outlined by Boyle et al. (2018), with modifications in the solubilization medium, volume of the sample solution, volume of corn oil, and the homogenizer used. Protein solutions (0.1% protein, w/v) were prepared, in triplicate, either in DDW or 0.5 M NaCl, and solubilized for 2 h before the pH was adjusted to 7.0. An aliquot (5 mL) was added to 1.67 mL of corn oil and homogenized at 18,000 rpm for 1 min using an IKA T-25 ULTRA-TURRAX® high shear homogenizer (IKA Works, Inc., Wilmington, NC, USA). An aliquot (50 μL) of the homogenized emulsion was added to 0.1% SDS and initial absorbance was measured at 500 nm using a UV/VIS spectrophotometer (Beckman Coulter DU 800, Brea, CA, USA). After 10 min, another aliquot (50 μL) of the emulsion was added to 0.1% SDS and the absorbance was measured. The ES (min) and EAI (m^2 g^{-1}) were calculated as reported by Boyle et al. (2018).

2.8. Amino acid composition and nutritional quality of hemp protein isolates

2.8.1. Amino acid composition

Amino acids were hydrolyzed according to the AOAC official method 982.30, and cysteine and methionine were hydrolyzed using performic acid oxidation per the AOAC official method 994.12. Tryptophan was determined using alkaline hydrolysis as described by Nosworthy et al. (2017). Amino acid composition was used to calculate the amino acid score (AAS) and the nitrogen conversion factor of each HPI sample, where the reference amino acid is that which is required for preschool children ages 2–5 years as defined by FAO/WHO Expert Consultation.

2.8.2. In vitro protein digestibility and protein digestibility-corrected amino acid score (PDCAAS)

In vitro protein digestibility of the HPI samples was measured using the pH drop method as outlined by Franczyk (2018), based on the method developed by Hsu et al. (1977) and modified by Tinus et al. (2012). The enzyme solution was prepared by weighing 1.6 mg trypsin, 3.1 mg chymotrypsin, and 1.3 mg peptidase for each mL of solution required. The enzyme solution was stirred and heated to 37 °C (±1 °C) in a water bath for 10 min. The pH was adjusted to 8.0 ± 0.05 and placed in an ice bath to cool to 0–4 °C. In triplicate, protein samples were dispersed (62.5 mg ± 3 mg of crude protein) in 10 mL Milli-Q water. Sample solutions were stirred and heated to 37 °C in a water bath for 1 h, or until there were no clumps present. The pH was again adjusted to 8.0 ± 0.05. The exact starting pH of each sample solution was recorded, and the enzyme solution (1 mL) was immediately added. After 10 min, the final pH of the sample solution was recorded. Casein was run as a control alongside the HPI samples to assure consistency of the results. *In vitro* protein digestibility was calculated based on the change in pH. Protein digestibility-corrected amino acid score (PDCAAS) for the HPI samples was then calculated based on the AAS and *in vitro* protein digestibility measurements.

2.9. Percent theoretical amino acid distribution and homology among soy and hemp 11S and 7S globulins

Multiple Sequence Alignment (MSA) and percent homology analysis were conducted with Clustal Omega (https://www.ebi.ac.uk/Tools/msa/clustalo/) using various subunits and genetic variants of soy and hemp 11S and 7S globulins, which were downloaded from Uniprot (https://www.uniprot.org/). The theoretical amino acid distribution of different genetic variants of 11S edestin and 7S vicilin-like protein was assessed using ProtParam (https://web.expasy.org/protparam). Accession numbers for each subunit from Uniprot are listed in Table S1.

2.10. Statistical analysis

Analysis of variance (ANOVA) was performed using RStudio Version March 1, 1073 for Windows (RStudio, Boston, MA, USA). Tukey-Kramer multiple means comparison test was used to determine significant differences ($P \leq 0.05$) among the means (n ≥ 3) of three or more samples. A student's unpaired *t*-test was used to determine significant differences ($P \leq 0.05$) between the means of two samples.

3. Results and discussion

3.1. pH extraction of hemp protein

Hemp protein is soluble under a relatively high alkalinity, where the net negative charge is sufficiently high, above its isoelectric point (pH 5–6) (Girgih et al., 2014; Hadnađev et al., 2018; M. Liu et al., 2023; X. Liu et al., 2023; Shen et al., 2020). The higher extractability at high alkalinity has been attributed to the enhanced solubilization of edestin, which makes up 60–80% of the proteins in hemp (Malomo and Aluko, 2015b). However, solubilization under high alkalinity results in protein denaturation, and contributes to undesirable browning due to oxidation of polyphenols that are abundant in the hemp hulls (Shen et al., 2020). Therefore, hemp protein was extracted at different pHs to evaluate the impact on protein purity, yield, color, and protein characteristics.

Hemp protein demonstrated low extractability between pH 7–9 (Fig. 1A). Significantly higher solubilization was noted at pH 10 and more so at pH 11, while pH 12 did not contribute to further enhancement in protein extractability. The majority of the protein, 60–80%, were extracted at pH 10 and 11. In contrast, Potin and Saurel (2020) and Helstad et al. (2022) reported a significant increase in the extent of protein solubilization with the increase in pH, up to pH 12. This discrepancy could be attributed to the absence of hulls in the DHM

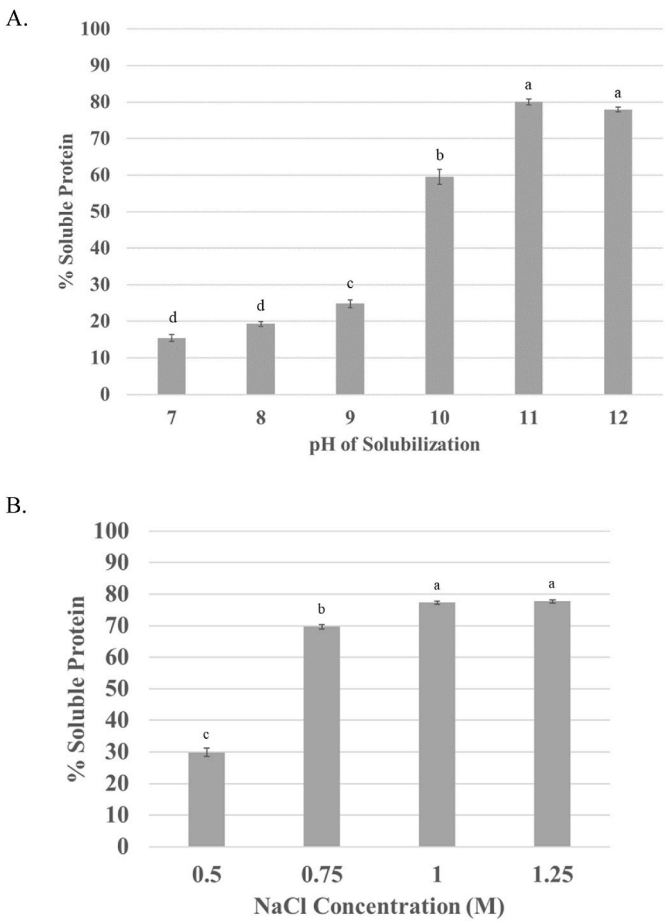

Fig. 1. % Soluble protein at different solubilization pHs (A) and at different salt (NaCl) concentrations when heated at 50 °C (B). Error bars represent standard error (n = 3). Different lowercase letters above the bars indicate significant differences among the samples according to the Tukey-Kramer multiple means comparison test ($P < 0.05$).

produced in this study compared to the non-dehulled hempseed press-cake used as the starting material by Potin and Saurel (2020) and Helstad et al. (2022). Hulls could impede protein extraction due to entanglement with fibrous material. Extremely high alkalinity can breakdown the fiber components and enhance extractability of the protein. Accordingly, protein extraction to produce HPI from the dehulled DHM was performed at both solubilization pHs, pH 10 and 11, followed by precipitation at pH 5. Precipitation at pH 5 was based on previous reports (Girgih et al., 2014; Hadnađev et al., 2018; M. Liu et al., 2023; X. Liu et al., 2023; Shen et al., 2020).

The significantly higher protein solubility at pH 11 compared to pH 10 contributed to a significantly higher (>20%) yield for pH-HPI (Table 1). Over 87% of the protein was extracted at pH 11, while about 25% of the protein remained in the residue after solubilization at pH 10. Double solubilization with replenishing of the alkaline solution contributed to the enhanced extraction compared to single solubilization (Fig. 1A). Most of the solubilized protein, at both pH 10 and 11, was precipitated at pH 5, with a minor statistical difference. The observed protein purity was comparable to previous reports, while the protein yield was markedly higher than reported values (37.9–73.0%), where the protein was extracted at pH 10–12 (Hadnađev et al., 2018; Helstad et al., 2022; Shen et al., 2020; Tang et al., 2006; Wang et al., 2018). The relatively high yield observed could be attributed not only to the double solubilization employed uniquely in this study, but also to the use of DHM produced from dehulled seeds.

Shen et al. (2020) demonstrated a higher protein purity and yield of

Table 1
Protein purity and yield as affected by the solubilization pH following alkaline extraction coupled with isoelectric precipitation.

Solubilization pH	HPI[a]			Discarded Pellet[b]		Discarded Supernatant[c]	
	Protein Purity (%)	Protein Yield (%)	Ash (%)	Protein Purity (%)	Protein Residue (%)	Protein Purity (%)	Protein Lost (%)
10	84.8	64.2	1.75	45.2*	25.0*	30.2	7.39
11	88.1*	87.3*	2.37*	3.92	1.23	29.1	11.1*

Protein purity (%) represents the amount of protein in the lyophilized sample as determined by the Dumas method; Protein yield (%) represents the amount of protein extracted relative to the total amount of protein in the starting defatted hemp meal (DHM); Protein residue (%) represents the amount of protein left in the discarded pellet relative to the total amount of protein in the starting DHM; Protein lost (%) represents the amount of protein lost in the discarded supernatant relative to the total amount of protein in the starting DHM. An asterisk (*) indicates a significant difference in each column as tested by the student's unpaired *t*-test ($P < 0.05$).
[a] HPI – Hemp protein isolate.
[b] Pellet discarded after alkaline solubilization.
[c] Supernatant discarded after isoelectric precipitation.

HPI produced via AE-IEP (pH 10) from dehulled seeds (91.1% protein purity, 46.9% protein yield) than from non-dehulled seeds (82.2% protein purity, 39.3% protein yield). Similarly, Tang et al. (2006) reported an even higher protein yield (73.0%) following AE-IEP (pH 10) from dehulled hemp seeds. Apart from fiber entanglement issues, the phenolic compounds, concentrated in the hulls, are oxidized under high alkalinity inducing protein polymerization, which in turn decrease protein solubility (Ozdal et al., 2013). In addition to decreasing protein extraction yields, protein polymerization may have a negative impact on protein quality and functionality (Ozdal et al., 2013; Potin et al., 2019; Zhang et al., 2021). Nevertheless, due to relatively high yield and purity, solubilization at pH 11 coupled with precipitation at pH 5 were selected as the AE-IEP conditions to produce pH-HPI from dehulled DHM for structural and functional characterization.

3.2. Salt extraction of hemp protein

When comparing protein extractability from DHM at different salt concentrations, hemp protein was significantly the least soluble at 0.5 M NaCl (Fig. 1B). While significantly more protein was solubilized at 1 M NaCl compared to 0.75 M, the difference was less than 10%. Any salt added during protein extraction needs to be removed from the final protein isolate to avoid adverse effects on protein functionality. The removal of salt requires multiple water washes, generating a large amount of waste stream and high expenditure of water, thus limiting industrial feasibility. Accordingly, and considering the relatively small difference in solubility, solubilization at 0.75 M instead of 1 M NaCl was further evaluated against 0.5 M.

The significantly higher protein extractability at 0.75 M compared to 0.5 M NaCl resulted in a significantly higher (>30%) yield (Table 2), with a significantly lower residual protein in the discarded pellet.

Table 2
Purity and yield as effected by salt (NaCl) concentration following salt extraction at 50 °C coupled with ultrafiltration.

Salt Concentration (M)	HPI[a]			Discarded Pellet[b]	
	Protein Purity (%)	Protein Yield (%)	Ash (%)	Protein Purity (%)	Protein Residue (%)
0.5	82.7	50.3	8.38*	55.0*	40.9*
0.75	86.6*	81.6*	4.09	17.8	7.46

Protein purity (%) represents the amount of protein in the lyophilized sample as determined by the Dumas method; Protein yield (%) represents the amount of protein extracted relative to the total amount of protein in the starting defatted hemp DHM; Protein residue (%) represents the amount of protein left in the discarded pellet relative to the total amount of protein in the starting DHM. An asterisk (*) indicates a significant difference in each column as tested by the student's two-sample unpaired *t*-test ($P < 0.05$).
[a] HPI – hemp protein isolate.
[b] Pellet discarded after salt solubilization.

Similar to AE-IEP, SE-UF was successful in producing HPI with high protein purity and exceptionally high protein yield. The protein purity of salt-HPI is comparable to what has been reported for pea protein isolate (92.8%) and chickpea protein isolate (91.9 %) produced by SE-UF (Hansen et al., 2022; Yaputri et al., 2023). While Hadnađev et al. (2018) reported higher protein purity for their salt-extracted HPI using UF, the protein purity was reported on dry basis and a higher nitrogen conversion factor (5.7) was used compared to the more accurate one (5.3) used in this study. The protein yield reported by Hadnađev et al. (2018), however, was half that obtained in this study (40%). The higher yield observed in this study is attributed to double solubilization with fresh salt solution, and to a higher solubilization temperature (50 °C compared with 35 °C). When comparing the protein yield of salt-HPI to that of other protein isolates produced via SE-UF, it was notably greater than that reported for pea protein isolate (72 % protein yield) (Hansen et al., 2022) and chickpea protein isolate (52% protein yield) (Yaputri et al., 2023). This is the first study to show the potential of ultrafiltration in the production of HPI with a relatively high protein purity. Purification of salt extracted protein using ultrafiltration has been successfully scaled to pilot plant production for pea and chickpea protein, confirming industrial feasibility of such process (Hansen et al., 2022; Yaputri et al., 2023). Due to relatively high yield and purity, solubilization at 0.75 M was selected as to produce salt-HPI via SE-UF for structural and functional characterization in comparison to pH-HPI.

3.3. Effect of extraction method and cultivar on color of HPI

The color of pH and salt extracted HPI (CFX-2 2016 pH-HPI vs. CFX-2 2016 salt-HPI) was compared to that of commercial isolates, cSPI and cPPI (Table 3). Salt-HPI was the lightest and most neutral in color among the isolates. While pH-HPI had significantly higher L* than cSPI and cPPI, the difference is numerically small and might not be detectable to the naked-eye. The difference in lightness between salt-HPI and pH-HPI

Table 3
Color (L* a* b*) of commercial soy protein (cSPI), commercial pea protein (cPPI), pH-extracted and salt-extracted hemp protein isolates (CFX-2 2016 pH-HPI and CFX-2 2016 salt-HPI, respectively), and pH-extracted hemp protein isolates from four different industrial hemp cultivars (CFX-2 2019, Grandi, Joey, Picolo).

Protein Isolate	L*	a*	b*
cSPI	86.2^{b^*}	-0.21^{e}	$+14.8^{b}$
cPPI	86.6^{b}	$+0.22^{d}$	$+19.1^{a}$
CFX-2 2016 pH-HPI	82.8^{c}	$+0.28^{d}$	$+11.5^{f}$
CFX-2 2016 salt-HPI	91.9^{a}	-0.14^{e}	$+5.22^{g}$
CFX-2 2019 pH-HPI	79.8^{e}	$+1.23^{b}$	$+13.6^{d}$
Grandi pH-HPI	78.4^{f}	$+1.49^{a}$	$+14.8^{b}$
Joey pH-HPI	81.0^{d}	$+1.27^{b}$	$+14.5^{c}$
Picolo pH-HPI	82.6^{c}	$+1.01^{c}$	$+13.0^{e}$

ˆ Means (n = 3) in each column with different lowercase letters indicate significant differences in L*, a*, and b* across protein isolates according to the Tukey-Kramer multiple means comparison test ($P < 0.05$).

can be attributed to browning that could have occurred at the high alkalinity used during AE-IEP. Salt-HPI had a higher L* than previously reported for HPI (Galves et al., 2019; Hadnađev et al., 2018; Shen et al., 2020). In addition, pH-HPI had a higher L* value than that reported for HPI produced from non-dehulled hemp seeds, and a similar L* value to the HPI produced from dehulled hemp seeds (Tang et al., 2006). The reported dark color of HPI was attributed to the oxidation of polyphenols present in the hulls and seed coatings (Girgih et al., 2014; Hadnađev et al., 2018; Teh et al., 2014). The color results in this study provided further evidence that dehulling is a necessary step to avoid excessive browning during alkaline extraction.

All pH-HPI produced from the 4 cultivars (CFX-2, Grandi, Joey, and Picolo) had comparable color values, with minor statistical differences (Table 3). The differences in color among the pH-HPI samples could be attributed to inherent variability in pigmentation among the cultivars. Nevertheless, the relatively comparable color of all pH-HPI samples to commercial isolates and the light color of salt-HPI would potentially contribute to consumer acceptability in a variety of food applications.

3.4. Effect of extraction method and cultivar on protein structural characteristics

3.4.1. Protein profile

Relative to all HPI samples, cSPI and cPPI had higher molecular weight (>50 kDa) globulin proteins (Fig. 2), glycinin and β-conglycinin, and legumin and vicilin, respectively (Bu et al., 2022; Hansen et al., 2022). In addition, HPI samples appeared to have a relatively larger proportion of albumin proteins than both cSPI and cPPI. The relatively lower molecular weight globulins and the higher proportion of albumin proteins may have negative implications on functional properties.

Both pH-HPI and salt-HPI had similar protein components (Fig. 2A, lanes 4&5). Under non-reducing conditions, the intense protein band around 50 kDa corresponded to monomers of 11S edestin and overlapping subunits of 7S vicilin-like protein (Hadnađev et al., 2018; Wang et al., 2018). Another intense band around 12 kDa corresponded to 2S albumins. The protein bands close to 100 kDa, which were apparent under non-reducing conditions, were most likely dimers linked by disulfide bonds since they were not visible under reducing conditions (Fig. 2A, lanes 4&5 compared to lanes 8&9).

Under reducing conditions, two intense bands were observed in both pH-HPI and salt-HPI at ~35 and ~20 kDa, corresponding to the acidic and basic subunits of the 11S edestin monomer that is stabilized by disulfide linkages (Fig. 2A, Lanes 8–9). The presence of basic subunits of two different molecular weights (~18 and 20 kDa) has been previously reported (Hadnađev et al., 2018; Potin et al., 2019). The relatively faint band still visible at ~50 kDa corresponded to 7S vicilin-like protein. This globulin protein is known to be deficient in disulfide linkages and to be much less abundant than 11S edestin. About 5% of total hemp proteins are 7S vicilin-like protein, while ~60–80% are 11S edestin (Sun et al., 2021). The two polypeptide chains under 10 kDa were identified as 2S albumin subunits, and are commonly referred to as heavy and light chains (Aluko, 2017).

Under non-reducing conditions, cSPI and cPPI had intense banding and smearing in the upper region of the gel, indicating presence of protein polymers of molecular weights >250 kDa (Fig. 2A, lanes 2–3 and 6–7). The persistence of these bands under reducing conditions suggested the presence of a high proportion of protein aggregates stabilized by covalent linkages. Processing conditions can alter the inherent protein profile. Commercially produced protein isolates undergo heating during concentration, pasteurization, inactivation of antinutrients, and spray drying. Such thermal treatments cause protein denaturation and subsequent polymerization via hydrophobic and disulfide linkages resulting in the formation of large insoluble aggregates (Bu et al., 2022; Hansen et al., 2022).

On the other hand, high molecular weight banding and smearing was visible for pH-HPI but was less evident for salt-HPI (Fig. 2A, lanes 4&5).

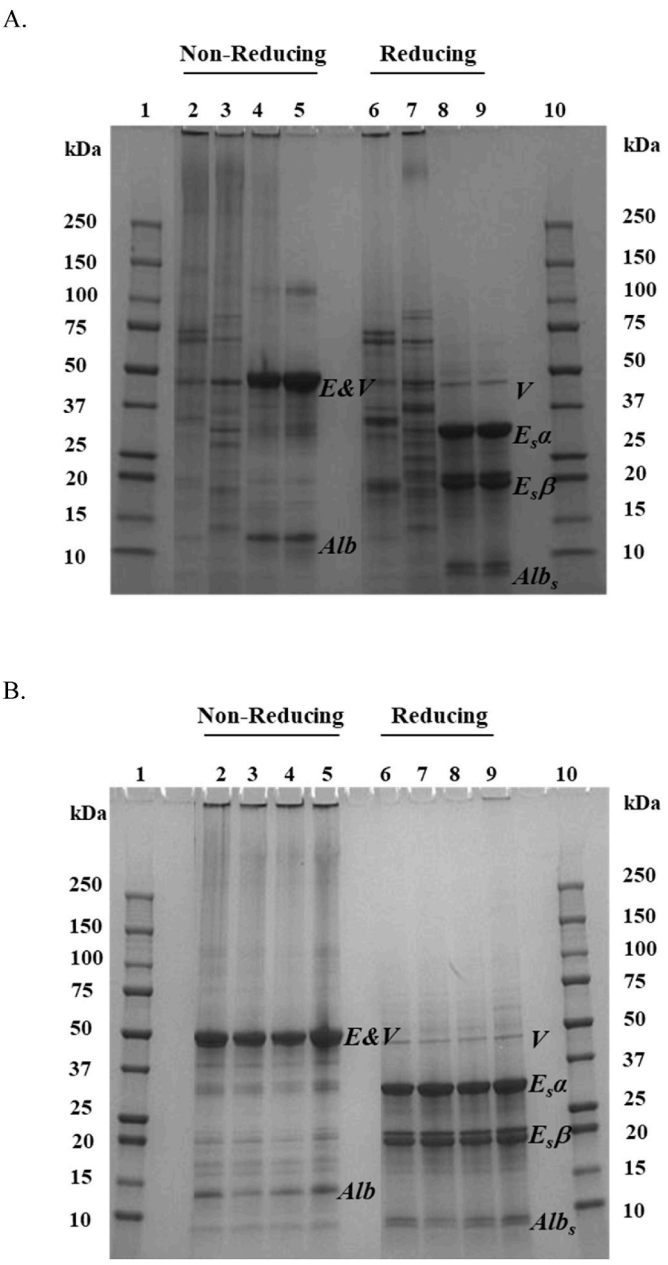

Fig. 2. SDS-PAGE visualization of the protein profiles of pH-extracted and salt-extracted hemp protein isolates (CFX-2 2016 pH-HPI and CFX-2 2016 salt-HPI) compared with commercially produced soy and pea protein isolates (cSPI and cPPI) (A) and of pH-extracted hemp protein isolates from different cultivars (CFX-2 2019 HPI, Grandi HPI, Joey HPI, Picolo HPI) (B) under non-reducing (lanes 2–5) and reducing (lanes 6–9) conditions. (A): Lane 1, 10: Molecular weight (MW) marker; Lane 2, 6: cSPI; Lane 3, 7: cPPI; Lane 4, 8: pH-HPI, Lane 5, 9: salt-HPI. (B): Lane 1, 10: Molecular weight (MW) marker; Lane 2, 6: CFX-2 2019 HPI, Lane 3, 7: Grandi HPI; Lane 4, 8: Joey HPI; Lane 5, 9: Picolo HPI. E: 11S edestin monomer; V: 7S vicilin-like protein monomer; Alb: 2S albumin; $E_s\alpha$: acidic subunit cleaved from edestin monomer; $E_s\beta$: basic subunit cleaved from edestin monomer; Alb_s: albumin subunits.

Under reducing conditions, the smearing disappeared, indicating that polymerization in HPI occurred via disulfide linkages (Fig. 2A, lanes 8&9). The higher extent of polymerization in pH-HPI compared to salt-HPI is attributed to the high alkalinity during AE-IEP. High alkalinity promotes denaturation and protein cross-linking, mostly via oxidation of the sulfhydryl groups. The relatively lower extent of polymerization observed for salt-HPI suggested that it had undergone less protein denaturation than pH-HPI, potentially impacting functional behavior.

There was no significant difference in the protein profile and intensity of the protein bands among pH-HPI samples from different cultivars (Fig. 2B). Despite this visual similarity in protein distribution among the four cultivars, other structural properties may be different, potentially leading to differences in functionality.

3.4.2. Protein denaturation

The lack of any endothermic peaks for cSPI and cPPI demonstrated that these protein samples were completely denatured (Table 4), which is consistent with previous reports (Bu et al., 2022; Hansen et al., 2022; Husband et al., 2024; Lee et al., 2003; Mitacek et al., 2023). Meanwhile, an endothermic peak, likely corresponding to the most dominant protein, edestin, was observed for all HPI samples, confirming that these proteins had not been completely denatured during extraction (Table 4). The observed denaturation temperature was slightly lower than the reported range of 89–95 °C (Hadnađev et al., 2018; Shen et al., 2020). Such difference compared to reported denaturation temperatures could be attributed to differences in salt content, with higher salt (or ash) content contributing to higher denaturation temperature (Añon et al., 2011). However, the enthalpy of denaturation fell within the reported range of 5–11 J g^{-1} for pH extracted HPI (Hadnađev et al., 2018; Shen et al., 2020). Similarly, one endothermic peak was observed for salt-HPI, however both the denaturation temperature and enthalpy were significantly higher than those of pH-HPI. The relatively milder extraction conditions of salt-HPI contributed to a better-preserved protein structure compared to pH-HPI. The lower enthalpy of denaturation for pH-HPI compared to salt-HPI indicated partial unfolding due to the high alkalinity during AE-IEP that contributed to the polymerization observed by SDS-PAGE (Fig. 2, lane 4 compared to 5). Partial unfolding may impact the surface properties of the protein and in turn its functional properties.

There were no major differences in the protein denaturation temperature among the pH-HPI samples from different cultivars. However, there were some significant differences in the enthalpy of denaturation, with Picolo pH-HPI having the highest value. Such difference could be attributed to some differences in amino acid composition, which in turn can lead to potential differences in the tertiary and quaternary structure of the protein.

Table 4
Denaturation temperatures and enthalpy, surface hydrophobicity, and surface charge of commercial soy protein (cSPI), commercial pea protein (cPPI), pH-extracted and salt-extracted hemp protein isolates (CFX-2 2016 pH-HPI and CFX-2 2016 salt-HPI, respectively), and pH-extracted hemp protein isolates from different cultivars (CFX-2 2019, Grandi, Joey, Picolo).

Samples	Denaturation Temperature	Enthalpy of Denaturation	Surface Hydrophobicity	Surface Charge
	Td, °C	ΔH, J g-1	RFI	mV
cSPI	~	~	9970^{a}	-46.5^{a*}
cPPI	~	~	12700^{a}	-36.9^{b*}
CFX-2 2016 pH-HPI	$77.5^{e\hat{}}$	6.94^{d}	20100^{ab}	-30.8^{c*}
CFX-2 2016 salt-HPI	91.0^{a}	19.2^{a}	18100^{b}	-25.6^{f*}
CFX-2 2019 pH-HPI	79.2^{c}	8.39^{c}	20010^{ab}	-27.5^{ef}
Grandi pH-HPI	79.7^{bc}	8.85^{cd}	22500^{a}	-28.8^{cde}
Joey pH-HPI	77.8^{d}	9.57^{c}	21300^{ab}	-28.4^{de}
Picolo pH-HPI	80.0^{b}	12.0^{b}	21400^{ab}	-29.9^{cd}

~ No peak of denaturation was observed; ^ Means (n ≥ 3) in each column with different lowercase letters indicate significant differences among samples according to the Tukey-Kramer multiple means comparison test ($P < 0.05$); Aa asterisk (*) indicates a significant difference between sample dissolved in DDW and in 0.5 M NaCl as tested by the student's unpaired t-test ($P < 0.05$). †N/A indicates that measurements were not taken under specified conditions.

3.4.3. Protein surface properties

All HPI samples had significantly higher surface hydrophobicity than cSPI and cPPI (Table 4). This observation aligns with findings by Galves et al. (2019) who reported higher surface hydrophobicity for hemp protein compared to other oilseed proteins. This high surface hydrophobicity could majorly impair protein solubility due to limited interactions with water. The minor difference in surface properties among the HPI from the four cultivars might not result in impactful differences in functional properties.

Surface charge is another important surface property impacting protein solubility and overall functionality. cSPI had a significantly higher net negative charge than cPPI (Table 4), which agrees with previous reports (Hansen et al., 2022; Husband et al., 2024). The net negative charge of all HPI samples was significantly lower than that of cSPI and cPPI and was in the range reported by Galves et al. (2019). The relatively lower net negative charge of salt-HPI compared to pH-HPI is most likely attributed to the higher ash content (Tables 1 and 2). Salt potentially can mask some of the charges on the surface of the protein. The minor variations in net charge observed among pH-HPI samples, all ranging between −27 and −30, may not have major implications on solubility. A net absolute charge above 30 mV is required for favorable protein-water interactions (Long and Labute, 2010). The relatively lower surface charge as well as higher surface hydrophobicity of all HPI samples compared to cSPI and cPPI indicate potentially lower protein-water interactions and consequently limited functionality.

3.4.4. Protein secondary structures

The protein secondary structure of cSPI and cPPI was primarily governed by intermolecular β-sheet (Fig. 3A and B). The harsh extraction conditions used during the production of these commercial ingredients, including high pH and thermal treatment, could have induced these intermolecular β-sheet structures, catalyzed by complete denaturation. Such intermolecular interactions can facilitate further molecular interactions, including disulfide linkages, which led to the formation of the observed aggregates (Fig. 2, lanes 2&3). In contrast, none of the HPI samples exhibited a significant intermolecular β-sheet peak (Fig. 3C–H). In addition, both cSPI and cPPI had much more prominent random coil peaks than the HPI samples. This observation confirmed that protein denaturation at the secondary level in the commercial samples is more than that in the produced HPI samples, in alignment with the extent of denaturation as assessed by DSC (Table 4).

While there were no noticeable differences in the secondary structure among the pH-HPI samples from different cultivars, the extraction method had an impact on the α-helix structure. It was apparent that AE-IEP contributed to less prominent α-helix structures in pH-HPI from all cultivars compared to salt-HPI (Fig. 3D compared to 3C and 3E-H). Similarly, Hadnađev et al. (2018) noted a lower abundance of α-helix in pH-extracted HPI compared to salt-extracted HPI. As discussed earlier, the high alkalinity resulted in partial denaturation, which could have contributed to reduction in α-helix structures. Differences in secondary structures between pH-HPI and salt-HPI compared to commercial samples may lead to functional disparities.

3.5. Effect of extraction method and cultivar on protein functional characteristics

3.5.1. Protein solubility

Solubility of the isolates was measured at pH 3.2 and 7 under non-heated and heated conditions to investigate their potential success in neutral and acidic beverage applications (Table 5). During preliminary testing, salt-HPI dispersed poorly in water and rapidly sedimented out of solution. Dispersing the salt-HPI in 0.5 M NaCl allowed for assessment of functionality without rapid sedimentation. Therefore, protein solubility

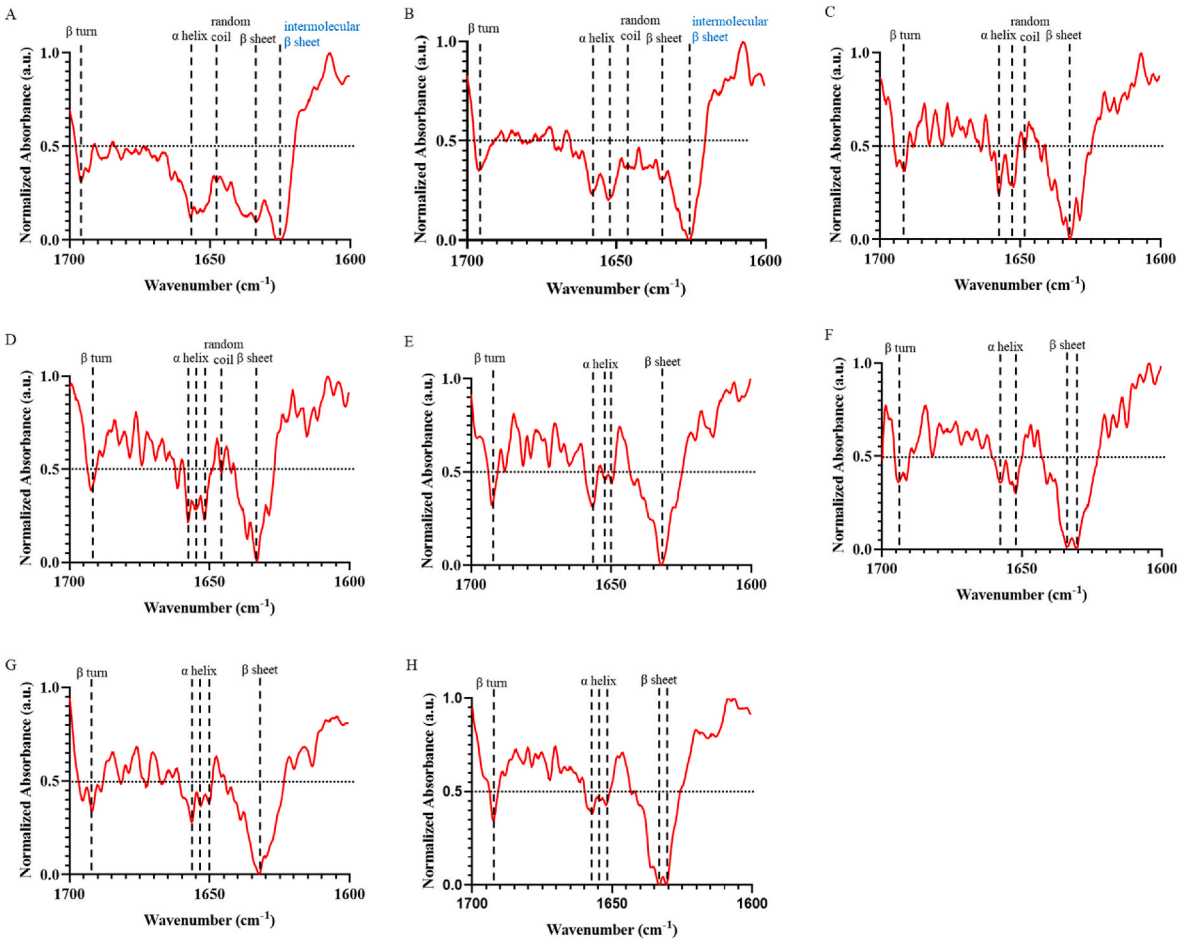

Fig. 3. Secondary protein structures of pH-extracted and salt-extracted hemp protein isolates (CFX-2 2016 pH-HPI and CFX-2 2016 salt-HPI, respectively), and pH-extracted hemp protein isolates from different cultivars (CFX-2 2019, Grandi, Joey, Picolo), compared with commercially produced soy and pea protein isolates (cSPI and cPPI). (A) cSPI; (B) cPPI; (C) CFX-2 2016 pH-HPI; (D) CFX-2 2016 salt-HPI; (E) CFX-2 2019 HPI; (F) Grandi HPI; (G) Joey HPI; (H) Picolo HPI.

Table 5
Solubility, gel strength, and water holding capacity of commercial soy protein (cSPI), commercial pea protein (cPPI), pH-extracted and salt-extracted hemp protein isolates (CFX-2 2016 pH-HPI and CFX-2 2016 salt-HPI, respectively), and pH-extracted hemp protein isolates from different cultivars (CFX-2 2019, Grandi, Joey, Picolo).

Samples	Solubility in DDW (1% protein)				Solubility in 0.5 M NaCl (1% protein)				Gel Strength (15% protein)		Water Holding Capacity	
	pH 7		pH 3.2		pH 7		pH 3.2		DDW	0.5 M NaCl	DDW	0.5 M NaCl
	Non-heated	Heated at 80 °C	Non-heated	Heated at 80 °C	Non-heated	Heated at 80 °C	Non-heated	Heated at 80 °C	Strength (N)	Strength (N)	%	%
cSPI	$67.8^{a\hat{}*}$	82.5^{a*}	52.9^{ab*}	65.2^{ab*}	26.6^{b}	28.6^{c}	16.6^{a}	18.8^{ab}	19.7^{c*}	8.91^{c}	99.8^{ab}	99.9^{a}
cPPI	41.8^{b}	60.1^{b*}	16.2^{c}	28.0^{c*}	24.4^{b}	34.1^{c}	13.4^{a}	14.5^{b}	2.07^{e}	~	99.9^{a}	~
CFX-2 2016 pH-HPI	15.5^{cd}	18.4^{c}	57.2^{ab*}	63.0^{ab*}	55.5^{a*}	57.0^{a*}	21.3^{a}	12.7^{b}	12.9^{d}	29.4^{b*}	86.6^{c*}	71.2^{c}
CFX-2 2016 salt-HPI	22.0^{c}	18.1^{cd}	55.0^{ab*}	61.5^{ab*}	45.0^{a*}	43.7^{b*}	22.7^{a}	23.3^{a}	~	$36.4^{\Psi a}$	~	81.4^{b}
CFX-2 2019 pH-HPI	7.5^{d}	11.2^{de}	55.9^{ab}	62.0^{ab}	N/A†	N/A	N/A	N/A	19.6^{c}	N/A	90.3^{c}	N/A
Grandi pH-HPI	9.2^{cd}	9.5^{e}	49.2^{b}	53.8^{b}	N/A	N/A	N/A	N/A	23.9^{a}	N/A	92.7^{bc}	N/A
Joey pH-HPI	8.9^{cd}	10.3^{e}	66.8^{a}	71.0^{ab}	N/A	N/A	N/A	N/A	21.7^{b}	N/A	91.0^{c}	N/A
Picolo pH-HPI	9.7^{cd}	10.7^{e}	66.6^{a}	71.6^{a}	N/A	N/A	N/A	N/A	23.2^{ab}	N/A	93.8^{abc}	N/A

$^{\hat{}}$ Means ($n \geq 3$) in each column with different lowercase letters indicate significant differences among samples according to the Tukey-Kramer multiple means comparison test ($P < 0.05$); An asterisk (*) indicates a significant difference between sample dissolved in DDW and in 0.5 M NaCl as tested by the student's unpaired *t*-test ($P < 0.05$); †N/A indicates that measurements were not taken under specified conditions; ~ No gels formed at 15% protein concentration under conditions specified in table; $^{\Psi}$ Salt-HPI gel formed in 0.5 M NaCl was not homogenous; bottom portion of gel was harder and upper portion of gel was softer.

for select isolates was evaluated in DDW and in 0.5 M NaCl solution.

At pH 7 in DDW, cSPI had the highest solubility, followed by cPPI, under heated and non-heated conditions (Table 5). The observed solubility of cSPI and cPPI is consistent with previous reports (Hansen et al., 2022; Yaputri et al., 2023). All HPI samples, regardless of extraction method or cultivar, had poor solubility at pH 7 in DDW, similar to previous reports (Hadnađev et al., 2018; Malomo and Aluko, 2015a; Shen et al., 2020). This observation is mostly attributed to the relatively high surface hydrophobicity to charge ratio (measured at pH 7) of all HPI samples relative to commercial isolates (Table 4). However, HPI samples exhibited much higher solubility at acidic pH, comparable to that cSPI and significantly higher than that of cPPI. The relatively higher solubility of HPI at pH 3.2 compared to pH 7 could potentially be attributed to higher net charge at this acidic pH. A greater absolute surface charge has been reported for HPI at pH 3 compared to pH 7 (Shen et al., 2020; Shen et al., 2020).

Dissolving both pH-HPI and salt-HPI in 0.5 M NaCl significantly enhanced their solubility at pH 7 yet reduced it significantly at pH 3.2 (Table 5). This opposite impact of salt on solubility at the two tested pHs could be attributed to increasing charge load at pH 7, and to shielding of surface charge at pH 3.2. In contrast, protein solubility of cSPI and cPPI was significantly lower in 0.5 M NaCl than in DDW under all conditions. Commercial soy protein isolates have demonstrated low solubility in 0.5 M NaCl, especially when complete denaturation was confirmed (Lee et al., 2003). Different proteins that vary in surface charge at a particular pH precipitate out at different salt concentrations. While it appeared that soy and pea were salted out, hemp protein was salted in at pH 7. While the salt at 0.5 M NaCl appeared to increase the charge load on the hemp protein, it in contrast shielded the charges on the surface of cSPI and cPPI. The impact of salt addition is dependent on the pH, which in turn dictates the ionization of the amino acid residues on the surface of the protein (Damodaran and Parkin, 2017).

The significant, yet minor, differences in surface charge among the HPI samples (Table 4) did not translate to differences in solubility at neutral pH. At pH 3.2, on the other hand, some differences in solubility among the four HPI samples were observed (Table 5). Grandi HPI had significantly lower solubility than Joey and Picolo HPI. The difference in solubility could not be explained by the noted structural properties (Table 4), but probably could be attributed to differences in amino acid composition. Joey and Picolo pH-HPIs had good solubility (>70%), similar to what has been reported for pH-extracted HPI at pH 3 (71.2%) measured at 1% total solids (Dapčević-Hadnađev et al., 2019). At pH 3.2, all four HPI samples demonstrated similar solubility to cSPI, which was an observation similar to the trend observed for both pH-HPI and salt-HPI (Table 5).

Overall, these results indicated that hemp protein could serve as a suitable alternative to soy protein in acidic beverages or could replace soy protein in high salt food applications where good protein solubility is desired at neutral pH. However, functionality of hemp protein in food systems at neutral pH, and relatively low ionic strength, may be limited, as good solubility is a precursor for other functional properties (Singh et al., 2008). Hemp varieties with more evident genetic variation need to be screened for structural differences that may contribute to improved solubility.

3.5.2. Gel strength and water holding capacity

Different protein concentrations were tested to determine the LGC for HPI. While the LGC for pH-HPI was 10% protein in water, salt-HPI would sediment out before heating in water, and no gel network could be formed at any protein concentration tested (up to 20% protein). However, the LGC of salt-HPI was determined to be 12.5% protein in 0.5 M NaCl. Therefore, to investigate the impact of extractions and cultivars on the water holding capacity and gel strength, 15% protein (in DDW and/or 0.5 M NaCl) was evaluated.

When dissolved in DDW, cSPI produced a strong gel, as expected, and consistent with previous reports (Hansen et al., 2022; Mitacek et al., 2023; Yaputri et al., 2023). On the other hand, also consistent with previous reports cPPI produced significantly weaker gels than cSPI (Hansen et al., 2022). pH-HPI, regardless of cultivars had a significantly higher gel strength than cPPI. In fact, the gel strength of Grandi, Joey, and Picolo was significantly higher than that of cSPI. This observation could be in part attributed to the high surface hydrophobicity (Table 4), partial denaturation (Table 4), and the presence of high molecular weight polymers (Figs. 1 and 2) in these samples. In contrast, salt-HPI precipitated before the gel network could fully form in water. This precipitation was attributed to the combination of low surface charge and high surface hydrophobicity of salt-HPI at pH 7 (Table 4), which most likely promoted strong protein-protein interactions at the high protein concentration used (15% protein) and consequent sedimentation. Moreover, salt-HPI had the highest denaturation temperature and enthalpy among the isolates (Table 4), possibly resulting in resistance to unfolding needed during the thermal treatment performed to induce a gel network formation.

When dissolved in 0.5 M NaCl, cSPI formed a weaker gel than in water, while cPPI did not form a gel (Table 5). This is in accordance with the observed reduced solubility in the salt solution. Due to enhanced solubility at pH 7, HPI gels were stronger in 0.5 M NaCl than in water (Table 5). The improved gel strength of HPI may be desirable in high-salt comminuted meat products such as frankfurters, which contain salt concentrations around 0.4 M NaCl (Sun and Arntfield, 2011). The demonstrated ability of HPI to cross-link could translate to good texturization potential, as proteins unfold and aggregate during texturization (Zhang et al., 2019). In fact, the pH-HPI gels produced had a more fibrous texture (Fig. S1) compared to cSPI and cPPI gels, which is desirable for texturization.

Water holding capacity (WHC) is another measure related to gelling ability as it indicates the ability to physically entrap water within the protein gel matrix. High WHC contributes to juiciness and tenderness in gel-type food applications, such as meat products or meat alternatives. There have been no previous reports on the WHC of HPI. When assessed in water, the WHC of the tested HPI samples was relatively high and comparable to that of cSPI and cPPI (Table 5), with minimal differences across cultivars. Solubilization in 0.5 M NaCl significantly reduced the WHC of pH- and salt-HPI. The addition of salt can cause formation of a gel network with potentially large pore sizes, contributing to syneresis (Dapčević-Hadnađev et al., 2018). Salt-HPI had significantly higher WHC than pH-HPI when the gel was prepared in 0.5 M NaCl, while minimal difference in WHC across different cultivars was observed. These observations indicated that pH-HPI can provide good WHC in gel-type food applications, while salt-HPI may provide good WHC in the presence of relatively higher salt content.

3.5.3. Emulsification properties

The emulsification properties of cSPI and cPPI were consistent with previous reports (Yaputri et al., 2023). In contrast, none of the HPI samples formed an emulsion when prepared in water at pH 7 (Table 6). This observation is mostly attributed to the poor solubility at neutral pH (Table 5), and potentially skewed balance of hydrophobic to charged residues on the surface of the protein (Table 4). When solubilized in 0.5 M NaCl, both HPI samples produced emulsions with EC values similar to that of the commercial samples. The enhanced solubility (Table 5) in 0.5 M NaCl allowed for the dispersed protein to reach the oil-water interface instead of falling out of solution. Interestingly, ES was significantly higher in HPI compared to the commercial samples with 0.5 M NaCl was the medium. Imparting a higher charge load on the surface of hemp protein in the presence of salt, while shielding charges on the surface of soy and pea protein, as discussed earlier, contributed to the observed differences in ES.

Salt-HPI demonstrated a significantly higher EC than pH-HPI, an observation that complemented previous findings based on oil droplet size. (Dapčević-Hadnađev et al., 2019) reported larger oil droplet sizes for pH-extracted HPI than salt-extracted HPI, concluding that

Table 6
Emulsification capacity, stability, and activity index of commercial soy protein (cSPI), commercial pea protein (cPPI), pH-extracted and salt-extracted hemp protein isolates (CFX-2 2016 pH-HPI and CFX-2 2016 salt-HPI, respectively), and pH-extracted hemp protein isolates from different cultivars (CFX-2 2019, Grandi, Joey, Picolo).

Samples	Emulsification Capacity (1% protein)		Emulsification Stability		Emulsification Activity Index	
	DDW	0.5 M NaCl	DDW	0.5 M NaCl	DDW	0.5 M NaCl
	g oil/g protein	g oil/g protein	min	min	m^2/g	m^2/g
cSPI	1194[a^*]	832[a]	11.5[a]	12.3[b]	144.8[a]	268.4[a*]
cPPI	777[b]	707[b]	12.5[a]	11.5[b]	185.5[a]	273.3[a*]
CFX-2 2016 pH-HPI	~	740[b]	~	30.9[a]	~	53.4[b*]
CFX-2 2016 salt-HPI	~	831[a]	~	26.1[a*]	~	71.2[b]
CFX-2 2019 pH-HPI	~	N/A[†]	~	N/A	~	N/A
Grandi pH-HPI	~	N/A	~	N/A	~	N/A
Joey pH-HPI	~	N/A	~	N/A	~	N/A
Picolo pH-HPI	~	N/A	~	N/A	~	N/A

[^] Means ($n \geq 3$) in each column with different lowercase letters indicate significant differences among samples according to the Tukey-Kramer multiple means comparison test ($P < 0.05$); An asterisk (*) indicates a significant difference between sample dissolved in DDW and in 0.5 M NaCl as tested by the student's unpaired *t*-test ($P < 0.05$); ~ All HPI samples did not form an emulsion at 1% protein when dissolved in DDW; [†]N/A indicates that measurements were not taken under specified conditions.

salt-extracted HPI had superior emulsifying properties. Nevertheless, hemp protein demonstrated inferior emulsification properties compared to soy and pea protein. Low solubility was determined to be the cause for hemp protein's underperformance as an emulsifier (Tang et al., 2006; Teh et al., 2014). When protein solubility is high (>50%), surface hydrophobicity has a larger impact on emulsification properties, whereas when protein solubility is low (<50%), solubility has a larger impact on emulsification properties (Li-Chan et al., 1984). However, results of this study highlighted the potential of improving the emulsification properties of HPI upon the addition of salt.

3.6. Effect of extraction method and cultivar on amino acid composition and nutritional quality

3.6.1. Amino acid composition of HPI samples and theoretical amino acid distribution of hemp protein variants

Evaluating the amino acid composition is crucial for determining the actual nitrogen conversion factor that is needed for accurate protein concentration measurement and is essential for assessing the nutritional quality of the different hemp protein samples. More importantly, the amino acid composition provides insights into the protein variants present in HPI samples.

The relatively high nitrogen percentages in certain amino acids can impact protein estimation and necessitates the calculation of the appropriate conversion factor based on amino acid composition (Table 7). Therefore, the calculated nitrogen conversion factor (5.30) for hemp protein, which deviated from the commonly employed 6.25, was used to accurately determine the protein content in the hemp protein samples and avoid overestimation. The calculated nitrogen conversion factor for both pH-HPI and salt-HPI was similar to that reported by the USDA (2018).

On the other hand, various extraction methods and cultivars may contribute to hemp protein isolates with varying ratios of its protein fractions, namely 11S edestin, 7S vicilin-like proteins and albumins. Such variation will result in differences in the amino acid composition. Therefore, the amino acid composition may offer additional insights into the observed differences in the functionality of HPIs. Accordingly, the amino acid composition of different HPIs was compared to the theoretical amino acid distribution of different genetic variants of 11S edestin (ede) and 7S vicilin-like protein monomers (Cs7S) obtained from the protein sequence database (Fig. 4, Supplemental Table 1). Additionally, the percentage of key (basic, acidic, sulfur-containing, hydrophobic, and critically hydrophobic) amino acids in different HPI samples was calculated and compared to that in different genetic variants of 11S edestin and 7S vicilin-like protein monomers (Table 7).

In hemp protein, Cs7S exhibits a significantly higher percentage of Lys compared to all three genetic variants of edestin (edestin 1, 2, and 3); whereas Arg in edestin is higher than that in Cs7S (Fig. 4 A). All HPI samples had a relatively high amount of Arg and a low proportion of Lys, indicating a dominant presence of edestin rather than Cs7S in all samples (Fig. 4 B), which is in alignment with the SDS-PAGE results (Fig. 2). Additionally, all HPI samples had a relatively high amount of Glu + Gln (>15%), likely due to the high relative abundance of edestin 3 in the samples, as edestin 3 contains a higher amount of Gln + Glu than other

Table 7
Percentage of key amino acids (g/100g protein) of pH-extracted and salt-extracted hemp protein isolates (CFX-2 2016 pH-HPI and CFX-2 2016 salt-HPI, respectively), and pH-extracted hemp protein isolates from different cultivars (CFX-2 2019, Grandi, Joey, Picolo).

Sample	Sulfur-containing AA[a] (%)	Acidic AA (%)	Basic AA (%)	Ratio of Acidic to Basic AA	Hydrophobic AA (%)	Critically Hydrophobic AA[b] (%)
CFX-2 2016 salt-HPI	3.83	30.9	21.2	1.46	34.7	20.3
CFX-2 2016 pH-HPI	4.31	29.8	20.7	1.44	36.1	21.2
CFX-2 2019 pH-HPI	3.82	30.0	20.5	1.46	36.4	21.4
Grandi pH-HPI	3.44	29.9	20.2	1.48	36.7	21.7
Joey pH-HPI	3.83	29.7	20.7	1.44	36.5	21.5
Picolo pH-HPI	3.76	29.7	20.2	1.47	36.6	21.6
Cs7S[c]	3.2	20.7	15.2	1.36	47.1	25.4
Ede[d]1A[e]	2.2	26.6	15.6	1.71	40.8	22.2
ede1B	2.2	26.6	15.5	1.72	40.8	22.2
ede1D	2.2	26.2	15.6	1.68	40.8	22
ede2A	3.8	26.1	15.2	1.72	43.7	22.6
ede2B	3.6	26.1	15.2	1.72	43.9	22.8
ede2C	3.8	26.1	15.2	1.72	43.9	22.8
CsEde[c]3A	5.2	26.3	13.9	1.89	44.3	22.6
CsEde3B	4	26.3	14.8	1.78	43.7	23.2

[a] Amino acids.
[b] Val, Leu, Ile, and Phe.
[c] 7S vicilin-like protein present in hemp.
[d] CsEde/ede: Edestin.
[e] 1A, 1B, 1C, 2A, 2B, 2C, 3A, and 3B, all are genetic variants of edestin. (Sequence information was obtained from Uniprot: https://www.uniprot.org/).

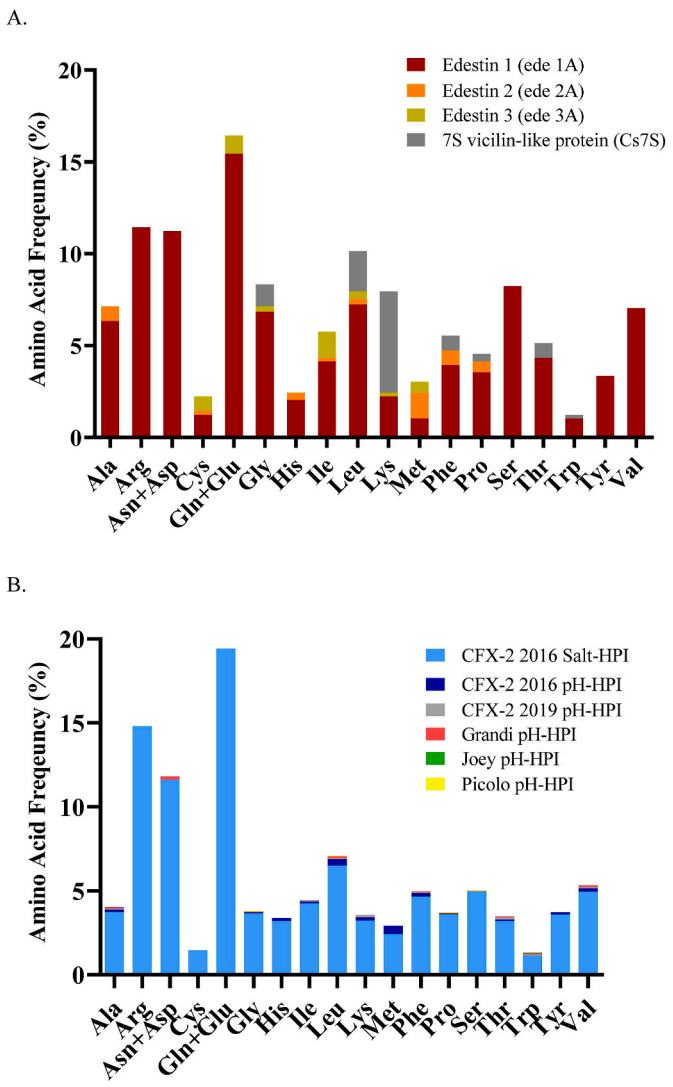

Fig. 4. Theoretical amino acid distribution of different genetic variants of 11S edestin and 7S vicilin-like protein monomers (A); and amino acid profile (g per 100 g protein, dry basis) of pH-extracted and salt-extracted hemp protein isolates (CFX-2 2016 pH-HPI and CFX-2 2016 salt-HPI, respectively), and pH-extracted hemp protein isolates from different cultivars (CFX-2 2019, Grandi, Joey, Picolo) (B). Color gradient represents extent of homology from 0 to 1, with lowest homology being the darkest red and highest homology being the darkest green.

edestin variants (Fig. 4). Meanwhile, the proportion of charged residues and the balance between acidic and basic amino acids influences the overall protein charge at a particular pH. The acidic to basic amino acids ratio of HPI fell within the range of that of Cs7s and all edestin variants (Table 7). A greater than 1 acidic to basic ratio at close to neutral pH contribute to net negative charge. In contrast, SPI has a relatively higher (~2) acidic to basic ratio (Hughes et al., 2011), which could partially explain the significantly higher negative charge compared to all HPI samples (Table 4).

In terms of sulfur containing amino acids, HPIs, especially CFX-2 2016 pH-HPI, had a relatively high content compared to the other HPI samples (Table 7). Edestin 1 contains less sulfur-containing amino acids than edestin 2 and 3. Therefore, all HPI samples possibly contained more edestin 2 and 3 than edestin 1, and CFX-2 2016 pH-HPI, specifically, contained more of edestin 3 than edestin 2. Sulfur-containing amino acids are involved in the formation of disulfide linkages, which can help in the formation of protein aggregates desirable for gelation or texturization (Tang et al., 2006). The sulfur-containing amino acids might have contributed to the ability of HPI samples to produce strong gels when solubility in the medium was sufficient to prevent sedimentation (Table 5).

Content of hydrophobic amino acids can also help explain protein functionality. The percentage of hydrophobic amino acids (Table 7) for Cs7S (47%) and edestin (40–44%) in hemp are higher than that of β-conglycinin (41%) and glycinin (39%) in soybean (Damodaran and Parkin, 2017), indicating that hemp protein in general is relatively more hydrophobic than soy protein, as was observed by the surface hydrophobicity data (Table 4). Of the hydrophobic amino acids, phenylalanine, leucine, isoleucine, and valine are critical because of their degree of hydrophobicity compared to other hydrophobic residues (Mo et al., 2006). If they comprise more than 28% of the total amino acids, hydrophobic interactions will offset any electrostatic repulsions among the protein molecules, resulting in protein aggregation and minimal solubility across a wide pH range. The percentages of these critical amino acids in all HPIs were below 28%, suggesting that surface hydrophobicity (Table 5) and solubility at pH 7 (Table 5) was mostly governed by total hydrophobic amino acids rather than the specific content of critically hydrophobic amino acid residues. It is important to note that Cs7S has relatively the highest percentage of critically hydrophobic amino acids (Table 7), which is higher than that (~22%) of soy 7S vicilin (Hughes et al., 2011). This fact might indicate that the role of Cs7S in the HPI might be different from that of the 7S vicilin in soy. Multiple sequence alignment also indicates low sequence homology (~25%) between 7S vicilin (Cs7S) in hemp and 7S β-conglycinin (GLCB1, GLCB2, GLCAP, GLCA2, GLCA1) in soy (Fig. 5, Supplemental Table 1).

On the other hand, 11 S edestin in hemp and 11S glycinin in soy share a relatively high sequence homology (approximately 45%) (Fig. 5, Supplemental Table 1). Edestin 1 and glycinin variants have the highest sequence homology, followed by edestin 3 and 2, indicating that the structure and functionality of edestin 1 could be closer to soy glycinin than those of edestin 2 and 3. In fact, the sequence homology among the edestin variants is only around 50%, suggesting considerable differences in protein structure and function among the edestin varients. For instance, within the edestin variants, the content of hydrophobic amino acids in edestin 2 and 3 is higher than that of edestin 1 (Table 7). In addition, edestin 1 contains fewer sulfur-containing amino acids, as discussed. Since edestin is the main protein present in HPI, hemp cultivars with significant genetic variation, should be studied and subjected to proteomics analysis to further understand the impact of edestin variants of the structure and functionality of hemp protein. Such work would aid breeding efforts in producing cultivars with targeted enhancement in functional properties for food applications.

3.6.2. *Nutritional quality*

One of the most fundamental roles of food proteins is providing nutritional value. Results confirmed that hemp protein is sufficient in arginine and the sulfur-rich methionine and cysteine, in higher amounts than that reported for soy and pea (Callaway, 2004; Hughes et al., 2011). Arginine may provide cardioprotective benefits, while methionine and cysteine are essential amino acids (House et al., 2010). Similar to other studies, lysine was determined to be the limiting amino acid in hemp (Fig. 4) and was used to calculate the amino acid score (Table 8).

pH-HPI had significantly higher *in vitro* digestibility than salt-HPI, which may be attributed to partial denaturation (Table 4). Partial denaturation can improve the digestibility of globular proteins, as unfolding can allow proteases better access to peptide bonds (Damodaran and Parkin, 2017). The higher *in vitro* digestibility of pH-HPI resulted in a significantly higher PDCAAS compared to salt-HPI. While the PDCAAS of HPI has not been reported previously, it fell within the range (0.48–0.61) reported by (House et al., 2010) for whole hemp seeds, dehulled hemp seeds, and hemp seed meal. The PDCAAS of both pH-HPI and salt-HPI is superior to that of other plant proteins such as wheat gluten (0.25), rice (0.53), and buckwheat (0.54) (Zeng et al., 2022). However, the PDCAAS of hemp protein is inferior to that of both

Sequence Identity	GLYG5	GLYG4	GLYG2	GLYG1	GLYG3	ede2B	ede2A	ede2C	ede1D	ede1B	ede1A	CsEde3A	CsEde3B	Cs7S	GLCB1	GLCB2	GLCAP	GLCA2	GLCA1
GLYG5	1.00	0.87	0.44	0.45	0.48	0.42	0.43	0.43	0.44	0.44	0.44	0.42	0.43	0.20	0.18	0.18	0.18	0.17	0.17
GLYG4	0.87	1.00	0.46	0.46	0.48	0.44	0.44	0.44	0.43	0.43	0.43	0.42	0.44	0.20	0.19	0.19	0.18	0.18	0.18
GLYG2	0.44	0.46	1.00	0.85	0.87	0.39	0.39	0.39	0.45	0.45	0.45	0.44	0.44	0.19	0.17	0.17	0.18	0.18	0.18
GLYG1	0.45	0.46	0.85	1.00	0.88	0.40	0.40	0.40	0.44	0.45	0.45	0.43	0.43	0.20	0.19	0.19	0.19	0.19	0.19
GLYG3	0.48	0.48	0.87	0.88	1.00	0.40	0.40	0.40	0.47	0.48	0.48	0.46	0.46	0.20	0.18	0.18	0.19	0.19	0.19
ede2B	0.42	0.44	0.39	0.40	0.40	1.00	1.00	1.00	0.50	0.50	0.50	0.49	0.50	0.22	0.22	0.22	0.19	0.18	0.18
ede2A	0.43	0.44	0.39	0.40	0.40	1.00	1.00	1.00	0.50	0.50	0.50	0.49	0.50	0.22	0.22	0.22	0.19	0.18	0.18
ede2C	0.43	0.44	0.39	0.40	0.40	1.00	1.00	1.00	0.50	0.50	0.50	0.50	0.50	0.22	0.22	0.22	0.19	0.18	0.18
ede1D	0.44	0.43	0.45	0.44	0.47	0.50	0.50	0.50	1.00	0.99	0.99	0.59	0.61	0.20	0.20	0.20	0.17	0.18	0.18
ede1B	0.44	0.43	0.45	0.45	0.48	0.50	0.50	0.50	0.99	1.00	1.00	0.59	0.61	0.21	0.20	0.20	0.18	0.18	0.18
ede1A	0.44	0.43	0.45	0.45	0.48	0.50	0.50	0.50	0.99	1.00	1.00	0.59	0.61	0.21	0.20	0.20	0.18	0.18	0.18
CsEde3A	0.42	0.42	0.44	0.43	0.46	0.49	0.49	0.50	0.59	0.59	0.59	1.00	0.92	0.22	0.18	0.18	0.17	0.17	0.17
CsEde3B	0.43	0.44	0.44	0.43	0.46	0.50	0.50	0.50	0.61	0.61	0.61	0.92	1.00	0.22	0.18	0.18	0.16	0.17	0.17
Cs7S	0.20	0.20	0.19	0.20	0.20	0.22	0.22	0.22	0.20	0.21	0.21	0.22	0.22	1.00	0.25	0.25	0.25	0.24	0.24
GLCB1	0.18	0.19	0.17	0.19	0.18	0.22	0.22	0.22	0.20	0.20	0.20	0.18	0.18	0.25	1.00	1.00	0.72	0.74	0.74
GLCB2	0.18	0.19	0.17	0.19	0.18	0.22	0.22	0.22	0.20	0.20	0.20	0.18	0.18	0.25	1.00	1.00	0.72	0.74	0.74
GLCAP	0.18	0.18	0.18	0.19	0.19	0.19	0.19	0.19	0.17	0.18	0.18	0.17	0.16	0.25	0.72	0.72	1.00	0.87	0.87
GLCA2	0.17	0.18	0.18	0.19	0.19	0.18	0.18	0.18	0.18	0.18	0.18	0.17	0.17	0.24	0.74	0.74	0.87	1.00	1.00
GLCA1	0.17	0.18	0.18	0.19	0.19	0.18	0.18	0.18	0.18	0.18	0.18	0.17	0.17	0.24	0.74	0.74	0.87	1.00	1.00

Fig. 5. Sequence identity of different genetic variants of 11S edestin and 7S vicilin-like protein monomers from hemp in comparison to 11S glycinin and 7S beta-conglycinin from soy.

Table 8
Amino acid score, *in vitro* digestibility, and calculated protein digestibility-corrected amino acid score (PDCAAS) of pH-extracted and salt-extracted hemp protein isolates (CFX-2 2016 pH-HPI and CFX-2 2016 salt-HPI, respectively), and pH-extracted hemp protein isolates from different cultivars (CFX-2 2019, Grandi, Joey, Picolo).

Sample	Amino Acid Score[a]	*In vitro* Digestibility (%)	PDCAAS
CFX-2 2016 salt-HPI	0.618	87.0^{b}	0.537^{d}
CFX-2 2016 pH-HPI	0.642	90.9^{a}	0.584^{c}
CFX-2 2019 pH-HPI	0.706	90.8^{a}	0.641^{a}
Grandi pH-HPI	0.684	91.8^{a}	0.628^{ab}
Joey pH-HPI	0.692	90.4^{a}	0.626^{ab}
Picolo pH-HPI	0.684	90.5^{a}	0.619^{b}

^ Means (n = 3) in each column with different lowercase letters indicate significant differences among samples according to the Tukey-Kramer multiple means comparison test ($P < 0.05$).

[a] Calculated using the recommended amino acid scoring pattern for children (2–5 years) (FAO/WHO Expert Consultation, 1991).

soy protein (0.92–1) and pea protein (0.73–0.89) (House et al., 2010; Hughes et al., 2011; Ismail et al., 2020; Singh et al., 2008). Nevertheless, hemp protein has similar digestibility to pea protein (82–85%) and soy protein (91–96%) (Han et al., 2007; Singh et al., 2008). As protein digestibility of both HPI is already quite high, an improvement in lysine content, potentially through breeding, could be a viable strategy to improve the overall nutritional value of hemp protein. It is worth noting that the amino acid scores of all HPI samples from 2019 cultivars were higher than that for CFX-2 2016 pH-HPI (Table 8). Therefore, it is also important to evaluate the effect of the growing, environmental, and storage conditions on the PDCAAS of hemp protein.

4Conclusions

Findings of this work demonstrated that both AE-IEP and SE-UF could be used to produce HPI with high protein purities and yields desirable for commercial production. Higher protein yields than previously reported for HPI were achieved with dehulling prior to defatting and protein extraction and through careful selection of protein extraction parameters. For the first time, a comprehensive characterization was performed to link the protein's structural properties to functionality and nutritional quality, as impacted by the extraction methods and cultivar. Comparing experimental amino acid composition to the theoretical amino acid distribution in hemp protein provided insights to the functional performance of the protein isolates. Results showed that AE-IEP resulted in a HPI that is more functional and nutritionally balanced than that produced following SE-UF. HPI demonstrated competitiveness to cSPI and cPPI in certain functional properties such as gelation at pH 7 and solubility at pH 3.2. There were minimal structural differences among HPI from the four cultivars, which contributed to only slight differences in functionality and nutritional quality. Based on HPI's poor solubility at neutral pH and lysine deficiency, future studies should focus on enhancing protein extractability under less adverse alkaline conditions and on evaluating HPI from cultivars that have wider genetic variance. Based on the theoretical analysis of amino acid composition, it appears that breeding hemp for targeted differences in edestin variants might lead to variation in protein functionality. Nevertheless, this work contributed to essential information that could guide future attempts to develop successful protein extraction processes, and to insights that could be valuable for breeding efforts, both targeted to enhance hemp protein characteristics for food applications.

CRediT authorship contribution statement

Laura Eckhardt: Conceptualization, Methodology, Data curation, Investigation, Formal data analysis, Writing – original draft. **Fan Bu:** Conceptualization, Methodology, Formal data analysis, Writing – review & editing. **Adam Franczyk:** Methodology, Data curation. **Tom Michaels:** Conceptualization, Resources. **Baraem P. Ismail:**

Conceptualization, Supervision, Project administration, Writing – review & editing, Funding acquisition.

Declaration of competing interest

The authors declare that they have no conflict of interest.

Data availability

Data will be made available on request.

Acknowledgements and Funding

This work was supported by funds from the Plant Protein Innovation Center, University of Minnesota. The authors also acknowledge James House for his help with facilitating the amino acid composition and digestibility analysis, Bühler for their help with dehulling the hemp seeds, Donn Vellekson for his help with separating the hemp hearts and hulls, Jason Neufeld for conducting the amino acid analysis, and Rachel Mitacek for helping with collecting the FTIR data.

Appendix A. Supplementary data

Supplementary data to this article can be found online at https://doi.org/10.1016/j.crfs.2024.100746.

References

Aluko, R., 2017. Hemp seed (Cannabis sativa L.) proteins: composition, structure, enzymatic modification, and functional or bioactive properties. In: Sustainable Protein Sources. Elsevier, pp. 121–132.

Añon, M.C., De Lamballerie, M., Speroni, F., 2011. Influence of NaCl concentration and high pressure treatment on thermal denaturation of soybean proteins. Innovat. Food Sci. Emerg. Technol. 12 (4), 443–450.

Barac, M., Cabrilo, S., Pesic, M., Stanojevic, S., Zilic, S., Macej, O., Ristic, N., 2010. Profile and functional properties of seed proteins from six pea (Pisum sativum) genotypes. Int. J. Mol. Sci. 11 (12), 4973–4990.

Boyle, C., Hansen, L., Hinnenkamp, C., Ismail, B.P., 2018. Emerging camelina protein: extraction, modification, and structural/functional characterization. J. Am. Oil Chem. Soc. 95 (8), 1049–1062.

Bu, F., Feyzi, S., Nayak, G., Mao, Q., Kondeti, V.S.K., Bruggeman, P., Chen, C., Ismail, B. P., 2023. Investigation of novel cold atmospheric plasma sources and their impact on the structural and functional characteristics of pea protein. Innovat. Food Sci. Emerg. Technol. 83, 103248.

Bu, F., Nayak, G., Bruggeman, P., Annor, G., Ismail, B.P., 2022. Impact of plasma reactive species on the structure and functionality of pea protein isolate. Food Chem. 371, 131135.

Cabral, E.M., Poojary, M.M., Lund, M.N., Curtin, J., Fenelon, M., Tiwari, B.K., 2022. Effect of solvent composition on the extraction of proteins from hemp oil processing stream. J. Sci. Food Agric. 102 (14), 6293–6298.

Callaway, J., 2004. Hempseed as a nutritional resource: an overview. Euphytica 140, 65–72.

Casey, R., Sharman, J.E., Wright, D.J., Bacon, J.R., Guldager, P., 1982. Quantitative variability in Pisum seed globulins: its assessment and significance. Plant Foods Hum. Nutr. 31, 333–346.

Damodaran, S., Parkin, K.L., 2017. Amino acids, peptides, and proteins. In: Fennema's Food Chemistry. CRC Press, pp. 235–356.

Dapčević-Hadnađev, T., Dizdar, M., Pojić, M., Krstonošić, V., Zychowski, L.M., Hadnađev, M., 2019. Emulsifying properties of hemp proteins: effect of isolation technique. Food Hydrocolloids 89, 912–920.

Dapčević-Hadnađev, T., Hadnađev, M., Lazaridou, A., Moschakis, T., Biliaderis, C.G., 2018. Hempseed meal protein isolates prepared by different isolation techniques. Part II. gelation properties at different ionic strengths. Food Hydrocolloids 81, 481–489.

Franczyk, A., 2018. Evaluation of in Vitro Methodology to Determine Protein Digestibility and Quality of Plant-Based Proteins.

Galasso, I., Russo, R., Mapelli, S., Ponzoni, E., Brambilla, I.M., Battelli, G., Reggiani, R., 2016. Variability in seed traits in a collection of Cannabis sativa L. genotypes. Front. Plant Sci. 7, 688.

Galves, C., Stone, A.K., Szarko, J., Liu, S., Shafer, K., Hargreaves, J., Siarkowski, M., Nickerson, M.T., 2019. Effect of pH and defatting on the functional attributes of safflower, sunflower, canola, and hemp protein concentrates. Cereal Chem. 96 (6), 1036–1047.

Girgih, A.T., He, R., Malomo, S., Offengenden, M., Wu, J., Aluko, R.E., 2014. Structural and functional characterization of hemp seed (Cannabis sativa L.) protein-derived antioxidant and antihypertensive peptides. J. Funct.Foods 6, 384–394.

Grand View Research, 2023. Protein ingredients market size, share and trends analysis report by product (plant proteins, animal/dairy proteins, microbe-based proteins, insect proteins), by application (foods & beverages), by region, and segment forecasts, 2023-2030. Retrieved July 3 from. https://www.grandviewresearch.com/industry-analysis/protein-ingredients-market.

Hadnađev, M., Dapčević-Hadnađev, T., Lazaridou, A., Moschakis, T., Michaelidou, A.-M., Popović, S., Biliaderis, C.G., 2018. Hempseed meal protein isolates prepared by different isolation techniques. Part I. physicochemical properties. Food Hydrocolloids 79, 526–533.

Han, I.H., Swanson, B.G., Baik, B.K., 2007. Protein digestibility of selected legumes treated with ultrasound and high hydrostatic pressure during soaking. Cereal Chem. 84 (5), 518–521.

Hansen, L., Bu, F., Ismail, B.P., 2022. Structure-function guided extraction and scale-up of pea protein isolate production. Foods 11 (23), 3773.

Helstad, A., Forsén, E., Ahlström, C., Mayer Labba, I.C., Sandberg, A.S., Rayner, M., Purhagen, J.K., 2022. Protein extraction from cold-pressed hempseed press cake: from laboratory to pilot scale. J. Food Sci. 87 (1), 312–325.

House, J.D., Neufeld, J., Leson, G., 2010. Evaluating the quality of protein from hemp seed (Cannabis sativa L.) products through the use of the protein digestibility-corrected amino acid score method. J. Agric. Food Chem. 58 (22), 11801–11807.

Housmans, J.A., Houben, B., Monge-Morera, M., Asvestas, D., Nguyen, H.H., Tsaka, G., Louros, N., Carpentier, S., Delcour, J.A., Rousseau, F., 2022. Investigating the sequence determinants of the curling of amyloid fibrils using ovalbumin as a case study. Biomacromolecules 23 (9), 3779–3797.

Hsu, H., Vavak, D., Satterlee, L., Miller, G., 1977. A multienzyme technique for estimating protein digestibility. J. Food Sci. 42 (5), 1269–1273.

Hughes, G.J., Ryan, D.J., Mukherjea, R., Schasteen, C.S., 2011. Protein digestibility-corrected amino acid scores (PDCAAS) for soy protein isolates and concentrate: criteria for evaluation. J. Agric. Food Chem. 59 (23), 12707–12712.

Husband, H., Ferreira, S., Bu, F., Feyzi, S., Ismail, B.P., 2024. Pea protein globulins: does their relative ratio matter? Food Hydrocolloids 148, 109429.

Irakli, M., Tsaliki, E., Kalivas, A., Kleisiaris, F., Sarrou, E., Cook, C.M., 2019. Effect of genotype and growing year on the nutritional, phytochemical, and antioxidant properties of industrial hemp (Cannabis sativa L.) seeds. Antioxidants 8 (10), 491.

Ismail, B.P., Senaratne-Lenagala, L., Stube, A., Brackenridge, A., 2020. Protein demand: review of plant and animal proteins used in alternative protein product development and production. Animal Frontiers 10 (4), 53–63.

Lee, K., Ryu, H., Rhee, K., 2003. Protein solubility characteristics of commercial soy protein products. J. Am. Oil Chem. Soc. 80 (1), 85–90.

Li-Chan, E., Nakai, S., Wood, D., 1984. Hydrophobicity and solubility of meat proteins and their relationship to emulsifying properties. J. Food Sci. 49 (2), 345–350.

Liu, M., Toth, J.A., Childs, M., Smart, L.B., Abbaspourrad, A., 2023. Composition and functional properties of hemp seed protein isolates from various hemp cultivars. J. Food Sci. 88 (3), 942–951.

Liu, X., Xue, F., Adhikari, B., 2023. Production of hemp protein isolate-polyphenol conjugates through ultrasound and alkali treatment methods and their characterization. Future Foods 7, 100210.

Long, W.F., Labute, P., 2010. Calibrative approaches to protein solubility modeling of a mutant series using physicochemical descriptors. J. Comput. Aided Mol. Des. 24, 907–916.

Malomo, S.A., Aluko, R.E., 2015a. A comparative study of the structural and functional properties of isolated hemp seed (Cannabis sativa L.) albumin and globulin fractions. Food Hydrocolloids 43, 743–752.

Malomo, S.A., Aluko, R.E., 2015b. Conversion of a low protein hemp seed meal into a functional protein concentrate through enzymatic digestion of fibre coupled with membrane ultrafiltration. Innovat. Food Sci. Emerg. Technol. 31, 151–159.

Mertens, C., Dehon, L., Bourgeois, A., Verhaeghe-Cartrysse, C., Blecker, C., 2012. Agronomical factors influencing the legumin/vicilin ratio in pea (Pisum sativum L.) seeds. J. Sci. Food Agric. 92 (8), 1591–1596.

Mitacek, R., Marks, M.D., Kerr, N., Gallaher, D., Ismail, B.P., 2023. Impact of extraction conditions and seed variety on the characteristics of pennycress (Thlaspi arvense) protein: a structure and function approach. J. Am. Oil Chem. Soc. 100 (11), 869–888.

Mo, X., Zhong, Z., Wang, D., Sun, X., 2006. Soybean glycinin subunits: characterization of physicochemical and adhesion properties. J. Agric. Food Chem. 54 (20), 7589–7593.

Nosworthy, M.G., Franczyk, A., Zimoch-Korzycka, A., Appah, P., Utioh, A., Neufeld, J., House, J.D., 2017. Impact of processing on the protein quality of pinto bean (Phaseolus vulgaris) and buckwheat (Fagopyrum esculentum Moench) flours and blends, as determined by in vitro and in vivo methodologies. J. Agric. Food Chem. 65 (19), 3919–3925.

Ozdal, T., Capanoglu, E., Altay, F., 2013. A review on protein–phenolic interactions and associated changes. Food Res. Int. 51 (2), 954–970.

Pannico, A., Kyriacou, M.C., El-Nakhel, C., Graziani, G., Carillo, P., Corrado, G., Ritieni, A., Rouphael, Y., De Pascale, S., 2022. Hemp microgreens as an innovative functional food: variation in the organic acids, amino acids, polyphenols, and cannabinoids composition of six hemp cultivars. Food Res. Int. 161, 111863.

Pesic, M.B., Vucelic-Radovic, B.V., Barac, M.B., Stanojevic, S.P., 2005. The influence of genotypic variation in protein composition on emulsifying properties of soy proteins. J. Am. Oil Chem. Soc. 82 (9), 667–672.

Potin, F., Lubbers, S., Husson, F., Saurel, R., 2019. Hemp (Cannabis sativa L.) protein extraction conditions affect extraction yield and protein quality. J. Food Sci. 84 (12), 3682–3690.

Potin, F., Saurel, R., 2020. Hemp seed as a source of food proteins. Sustain. Agric. Rev. 42: Hemp. Prod. Appl. 265–294.

Sadat, A., Joye, I.J., 2020. Peak fitting applied to fourier transform infrared and Raman spectroscopic analysis of proteins. Appl. Sci. 10 (17), 5918.
Shen, P., Gao, Z., Xu, M., Ohm, J.-B., Rao, J., Chen, B., 2020a. The impact of hempseed dehulling on chemical composition, structure properties and aromatic profile of hemp protein isolate. Food Hydrocolloids 106, 105889.
Shen, P., Gao, Z., Xu, M., Rao, J., Chen, B., 2020b. Physicochemical and structural properties of proteins extracted from dehulled industrial hempseeds: role of defatting process and precipitation pH. Food Hydrocolloids 108, 106065.
Singh, P., Kumar, R., Sabapathy, S., Bawa, A., 2008. Functional and edible uses of soy protein products. Compr. Rev. Food Sci. Food Saf. 7 (1), 14–28.
SPINS/GFI, 2023. U.S. retail market data for the plant-based industry. Retrieved July 3 from. https://gfi.org/marketresearch/#categories.
Sun, X., Sun, Y., Li, Y., Wu, Q., Wang, L., 2021. Identification and characterization of the seed storage proteins and related genes of cannabis sativa L. Front. Nutr. 8, 678421.
Sun, X.D., Arntfield, S.D., 2011. Dynamic oscillatory rheological measurement and thermal properties of pea protein extracted by salt method: effect of pH and NaCl. J. Food Eng. 105 (3), 577–582.
Tang, C.-H., Ten, Z., Wang, X.-S., Yang, X.-Q., 2006. Physicochemical and functional properties of hemp (Cannabis sativa L.) protein isolate. J. Agric. Food Chem. 54 (23), 8945–8950.
Teh, S.-S., Bekhit, A.E.-D., Carne, A., Birch, J., 2014. Effect of the defatting process, acid and alkali extraction on the physicochemical and functional properties of hemp, flax and canola seed cake protein isolates. J. Food Meas. Char. 8, 92–104.
Tinus, T., Damour, M., Van Riel, V., Sopade, P., 2012. Particle size-starch–protein digestibility relationships in cowpea (Vigna unguiculata). J. Food Eng. 113 (2), 254–264.
USDA, 2018. Seeds, hemp seed, hulled. In: FoodData Cent. Retrieved Oct 26 from. https://fdc.nal.usda.gov/fdcapp.html#/food-details/170148/nutrients.
Vonapartis, E., Aubin, M.-P., Seguin, P., Mustafa, A.F., Charron, J.-B., 2015. Seed composition of ten industrial hemp cultivars approved for production in Canada. J. Food Compos. Anal. 39, 8–12.
Wang, Q., Jin, Y., Xiong, Y.L., 2018. Heating-aided pH shifting modifies hemp seed protein structure, cross-linking, and emulsifying properties. J. Agric. Food Chem. 66 (41), 10827–10834.
Yaputri, B.P., Bu, F., Ismail, B.P., 2023. Salt solubilization coupled with membrane filtration-impact on the structure/function of chickpea compared to pea protein. Foods 12 (8), 1694.
Zeng, Y., Chen, E., Zhang, X., Li, D., Wang, Q., Sun, Y., 2022. Nutritional value and physicochemical characteristics of alternative protein for meat and dairy—a review. Foods 11 (21), 3326.
Zhang, J., Liu, L., Liu, H., Yoon, A., Rizvi, S.S., Wang, Q., 2019. Changes in conformation and quality of vegetable protein during texturization process by extrusion. Crit. Rev. Food Sci. Nutr. 59 (20), 3267–3280.
Zhang, Q., Cheng, Z., Wang, Y., Fu, L., 2021. Dietary protein-phenolic interactions: characterization, biochemical-physiological consequences, and potential food applications. Crit. Rev. Food Sci. Nutr. 61 (21), 3589–3615.